# Use of landslides for paleoseismic analysis

Randall W. Jibson

*US Geological Survey, Branch of Earthquake and Landslide Hazards, Box 25046, MS 966, Denver Federal Center, Denver, CO 80225, USA*

## Abstract

In many environments, landslides preserved in the geologic record can be analyzed to determine the likelihood of seismic triggering. If evidence indicates that a seismic origin is likely for a landslide or group of landslides, and if the landslides can be dated, then a paleo-earthquake can be inferred, and some of its characteristics can be estimated. Such paleoseismic landslide studies thus can help reconstruct the seismic history of a site or region. In regions that contain multiple seismic sources and in regions where surface faulting is absent, paleoseismic ground-failure studies are valuable tools in hazard and risk studies that are more concerned with shaking hazards than with interpretation of the movement histories of individual faults. Paleoseismic landslide analysis involves three steps: (1) identifying a feature as a landslide, (2) dating the landslide, and (3) showing that the landslide was triggered by earthquake shaking. This paper addresses each of these steps and discusses methods for interpreting the results of such studies by reviewing the current state of knowledge of paleoseismic landslide analysis.

## 1. Introduction

Most moderate to large earthquakes trigger landslides. In many environments, landslides preserved in the geological record can be analyzed to determine the likelihood of seismic triggering. If evidence indicates that a seismic origin is likely for a landslide or group of landslides, and if the landslides can be dated, then a paleo-earthquake can be inferred and some its characteristics can be estimated. Such paleoseismic landslide studies thus can help reconstruct the seismic shaking history of a site or region.

Paleoseismic landslide studies differ fundamentally from paleoseismic fault studies. Whereas fault studies seek to characterize the movement history of a specific fault, landslide studies characterize the shaking history of a site or region irrespective of the earthquake source. In regions that contain multiple seismic sources and in regions where surface faulting is absent, paleoseismic ground-failure studies thus can be valuable tools in hazard and risk studies that are more concerned with shaking hazards than with interpretation of the movement histories of individual faults.

As will be discussed in this paper, the practical lower-bound earthquake that can be interpreted from paleoseismic landslide investigations is about magnitude 5–6. This range is comparable or perhaps slightly lower than that for paleoseismic fault studies. Obviously, however, larger earthquakes tend to leave much more abundant and widespread evidence of landsliding than smaller earthquakes; thus, available evidence and confidence in interpretation increase with earthquake size.

Paleoseismic landslide analysis involves three

steps: (1) identifying a feature as a landslide, (2) dating the landslide, and (3) showing that the landslide was triggered by earthquake shaking. This paper addresses each of these steps and discusses methods for interpreting the results of such studies by reviewing the current state of knowledge of paleoseismic landslide analysis.

## 2. Identifying landslides

Landslides include many types of movement of earth materials. In this paper, the classification system of Varnes (1978) is used, which categorizes landslides by the type of material involved (soil or rock) and by the type of movement (falls, topples, slides, slumps, flows, or spreads). Other modifiers commonly are used to indicate velocity of movement, degree of internal disruption, state of activity, and moisture content (Varnes, 1978).

Identifying surface features as landslides can be relatively easy for fairly recent, well developed, simple landslides. Older, more degraded landslides or slides having complex or unusual morphologies are more difficult to identify. Several excellent summaries of approaches to landslide identification and investigation have been published (Schuster and Krizek, 1978; Záruba and Mencl, 1982; Brunsden and Prior, 1984; McCalpin, 1984), and the details need not be repeated here. In general, landslides are identified by anomalous topography, including arcuate or linear scarps, backward rotated masses, benched or hummocky topography, bulging toes, and ponded or deranged drainage. Abnormal vegetation type or age also are common. Submarine landslides can be identified with the aid of marine remote-sensing techniques (Field et al., 1982).

Earthquakes can trigger all types of landslides, and all types of landslides triggered by earthquakes also can occur without seismic triggering. Therefore, an earthquake origin cannot be determined solely on the basis of landslide type. However, some types of landslides tend to be much more abundant in earthquakes than other types. For example, Solonenko (1977) described some common characteristics of landslides triggered by earthquakes in the former Soviet Union. In a more comprehensive study, Keefer (1984) ranked the relative abundance of various types of landslides from 40 major earthquakes throughout the world (Table 1). Overall, more disrupted types of landslides are much more abundant than more coherent types of landslides. The relative rarity of subaqueous landslides stems, in part, from difficulties in observation. Keefer (1984) also observed that most earthquake-induced landslides occur in intact materials rather than in pre-existing landslide deposits; thus, the number of reactivated landslides is small compared to the total number of landslides triggered by earthquakes. Keefer (1984) described typical properties of source areas of various types of earthquake-triggered landslides. In general, slope materials that are weathered, sheared, intensely fractured or jointed, or saturated are particularly susceptible to landsliding during earthquakes.

Sackungen (ridge-crest troughs) are a somewhat controversial type of ground failure that some investigators claim may be related to seismic shaking. Sackungen are identified by one or more of the following: (1) grabens or troughs near and parallel to ridge crests of high mountains, (2) uphill-facing scarps a few meters high that parallel the topography, (3) double-crested ridges, and (4) bulging lower parts of slopes (Varnes et al., 1989).

Table 1
Relative abundance of earthquake-induced landslides

| Abundance | Landslide type |
|---|---|
| Very abundant | Rock falls |
| | Disrupted soil slides |
| | Rock slides |
| Abundant | Soil lateral spreads |
| | Soil slumps |
| | Soil block slides |
| | Soil avalanches |
| Moderately common | Soil falls |
| | Rapid soil flows |
| | Rock slumps |
| Uncommon | Subaqueous landslides |
| | Slow earth flows |
| | Rock block slides |
| | Rock avalanches |

Data from [Keefer (1984)]. Landslide types use nomenclature of [Varnes (1978)] and are listed in decreasing order of abundance.

## 3. Determining landslide ages

Paleoseismic interpretation requires establishing the numerical age of a paleo-earthquake. In the case of earthquake-triggered landslides, this means that dating landslide movement is required. Several methods for dating landslide movement can be used; some are similar or identical to those used for dating fault scarps, while others are unique to landslides. Most of the methods discussed below are simply modified applications of numerical dating techniques commonly used in other types of geological studies.

Different types of landslides may be datable by different methods, depending on a variety of factors such as distance of movement, degree of internal disruption, landslide geometry, type of landslide material, type and density of vegetation, and local climate. Ideally, multiple, independent dating methods should be used to increase the level of certainty of the age of landslide movement (Johnson, 1987).

### 3.1. Historical methods

Some old landslides may have been noted by local inhabitants or may have damaged or destroyed human works or natural features (e.g., Whitehouse and Griffiths, 1983). In some parts of the world, potentially useful historical records or human works may extend back several hundreds or thousands of years. For example, a prehistoric encampment at Mam Tor, in Derbyshire, England, was partly destroyed by a landslide (Johnson, 1987). The encampment was first occupied about 3000 years b.p. according to archaeological studies (Jones and Thompson, 1965); this date provides an approximate maximum age of the landslide. In the United States, few historical records exceed 200 years in length, but some of these may still be useful. In a paleoseismic investigation of landslides possibly triggered by the 1811–12 New Madrid earthquakes, Jibson and Keefer (1988) reported that oral accounts of local inhabitants helped establish minimum landslide ages in the 1850s, which helped bracket absolute ages. Also, grave markers on landslide masses, datable roads and trails whose locations clearly show that they either

postdated or predated landslide movement, disturbed stone fences or other property markers, and other human works can potentially bracket or definitively date landslide movement (e.g., Jibson and Keefer, 1988).

For fairly recent events, comparing successive generations of topographic maps or aerial photographs can bracket the time period in which mappable landslides first appeared.

### 3.2. Dendrochronology

Dendrochronology can be applied to date landslide movement in several ways (Hupp et al., 1987). At the simplest level, the oldest undisturbed trees on disrupted or rotated parts of landslides should yield reasonable minimum ages for movement (Jibson and Keefer, 1988; Logan and Schuster, 1991; Williams et al., 1992). On rotational slides that remained fairly coherent, preexisting trees that survived the sliding will have been tilted because of headward rotation of the ground surface; if both tilted and straight trees are present on such landslides, the age of slide movement is bracketed between the age of the oldest straight trees and the youngest tilted trees (Fuller, 1912). Using this simple application of dendrochronology to date coherent translational slides is more difficult because trees can remain upright and intact even after landslide movement. On all types of landslides, trees growing from the surface of the scarp will yield minimum ages of scarp formation, from which the age of slide movement can be interpreted.

In some cases, trees killed by landslide movement will be preserved and can thus yield the exact date of movement. For example, Jacoby et al. (1992) dated trees beneath the surface of Lake Washington near Seattle that were drowned by landsliding into the lake. They were able to date the landslide movement from the preserved tree-ring records and from radiocarbon dating of the outermost wood.

A more sophisticated application of dendrochronology involves quantitative analysis of growth rings. For trees that have survived one or more episodes of landslide movement, such analysis can be used to identify and date reaction wood

(eccentric growth rings), growth suppression, and corrosion scars, which may be evidence of landslide movement (Hupp et al., 1987). Reconstruction of movement histories by such dendrochronological analysis has been documented successfully in several areas (e.g., Terasmae, 1975; Reeder, 1979; Jensen, 1983; Bégin and Filion, 1985; Hupp et al., 1987; Osterkamp and Hupp, 1987).

Some landslides block stream drainages and form dams that impound ponds or lakes. Inundation of areas upstream from landslide dams can drown trees that can be dated dendrochronologically (Logan and Schuster, 1991).

### 3.3. Radiocarbon dating

Radiocarbon dating can be used in a variety of ways to date organic material buried by landslide movement, as discussed by Stout (1977). Landslide scarps degrade similarly to fault scarps, so colluvial wedges at the bases of landslide scarps may contain organic material that can be retrieved by trenching or coring and dated radiometrically. Fissures on the body of a landslide, particularly near the head where extension may take place, also may trap and preserve organic matter. If the landslide mass is highly disrupted, as in rock or soil falls or avalanches, then some vegetation from the original ground surface may have become mixed with the slide debris; such organic material excavated from slide debris can be dated radiometrically (Burrows, 1975; Whitehouse and Griffiths, 1983; McCalpin, 1989, 1992). At the toes of landslides, slide material commonly is deposited onto undisturbed ground; if this original ground surface can be excavated beneath the toe of a slide, buried organic material from this surface can be dated to indicate the age of initial movement.

Sag ponds commonly form on landslides, and organic material deposited in such ponds can be dated radiometrically. Organics at the base of the pond deposits should yield reliable dates of pond formation (Stout, 1969, 1977; McCalpin, 1989).

Vegetation submerged from inundation of areas upstream from landslide dams also can be dated radiometrically. Schuster et al. (1992) dated the emplacement of rock-avalanche dams by radiocarbon dating the outer few rings of drowned trees

protruding from landslide-dammed lakes and detrital wood and charcoal in lacustrine deposits that formed behind a landslide dam. Similarly, landslides into lakes can submerge and kill vegetation that can be dated radiometrically (Jacoby et al., 1992).

### 3.4. Lichenometry

Lichenometry – analysis of the age of lichens based on their size – has been used successfully to date rock-fall and rock-avalanche deposits (Nikonov and Shebalina, 1979; Oelfke and Butler, 1985; Nikonov, 1988; Smirnova and Nikonov, 1990; Bull et al., 1991; Bull, 1996). By measuring lichen diameters on rock faces freshly exposed at the time of failure, numerical ages can be roughly estimated by assuming that lichens colonized the rock face in the first year after exposure. Because rock-fall and rock-avalanche deposits typically include abundant rocks having freshly exposed faces, numerous samples generally can be taken to create a database for the statistical analysis required by lichenometry. Lichenometric ages must be calibrated at sites of known historical age or by comparison with other numerical dating techniques. Lichenometric dating is subject to considerable uncertainty, however, because several decades may elapse before lichens colonize a fresh rock exposure, and lichens may never colonize unstable landslide deposits on very steep slopes (Oelfke and Butler, 1985).

### 3.5. Weathering rinds

For a given climate and rock type, measuring the thickness of weathering rinds can be used to date when rocks were first exposed at the ground surface (Chinn, 1981; Knuepfer, 1988). For rock falls and rock avalanches and for other landslides whose movement exposed rock fragments at the ground surface, measuring the thickness of weathering rinds can be used to date landslide movement (Whitehouse and Griffiths, 1983; McCalpin, 1989, 1992). Determining which rock surfaces were initially exposed at the time of landsliding can be difficult, but if a sufficiently large number of samples can be measured, consistent statistical

results of predominant ages that relate to landslide movement can be obtained.

## 3.6. Pollen analysis

Analysis of pollen in deposits filling depressions on landslides can yield both an estimated age of initial movement and, in some cases, a movement history through time (Franks and Johnson, 1964; Adam, 1975; Tallis and Johnson, 1980; Dietrich and Dorn, 1984; Johnson, 1987). Such analyses assume that sediment deposition and incorporation of pollen occur immediately following landslide movement and that local climatic and vegetation variation can be accounted for. Pollen samples from the buried ground surface beneath the toes of landslides also have the potential for use in dating landslide movement.

## 3.7. Geomorphic analysis

Landslides are disequilibrium landforms that will change through time more rapidly than surrounding terrain. By analyzing the degree of degradation of landslide features such as scarps, ridges, sags, and toes, relative ages can be assigned to various landslides (Schroder, 1970; McCalpin, 1986; Crozier, 1992). For example, McCalpin and Rice (1987) analyzed 1200 landslides in the Rocky Mountains and assigned each of them to one of four relative age groups based on morphology. Numerical age ranges for these groups were estimated based on correlation with other landslides in the Rocky Mountains that have similar morphologies and surface-clast weathering and for which $^{14}$C dates were available. Although the classification scheme of McCalpin and Rice (1987) was developed for the Rocky Mountains, similar schemes could be developed for other areas (Wieczorek, 1984).

Another example of relative dating by geomorphic analysis was developed in New Zealand by Crozier (1992), who identified distinct age groups of landslides based on degree of definition of landslide features, soil development, tephra cover, stream dissection, preservation of vegetation killed by movement, and drainage integration. Ranges of numerical ages for these groups were estimated

by dating organic material retrieved from representative landslides from each group.

Jibson and Keefer (1988) concluded that since a large group of landslides in the New Madrid seismic zone all appeared to have the same degree of geomorphic degradation, these landslides were contemporaneous. Other types of evidence (Jibson and Keefer, 1988, 1989, 1993) were then used to link the synchronous ages of these landslides to triggering by the 1811–12 New Madrid earthquakes.

Models of fault-scarp degradation also have potential application in landslide dating because landslide scarps should behave similarly to fault scarps. Several approaches to morphological fault-scarp dating have been proposed (e.g., Bucknam and Anderson, 1979; Nash, 1980; Mayer, 1984), all of which require calibration for various parameters such as climate and scarp material. Scarp degradation commonly is modeled as a diffusion process (Colman and Watson, 1983; Andrews and Hanks, 1985; Andrews and Bucknam, 1987), in which degradation rate varies in time and is a function of slope angle, which represents the degree to which the scarp is out of equilibrium with the surrounding landscape.

Christiansen (1983) used sedimentation rates to date landslide age. An ancient landslide moved over alluvium deposited by the North Saskatchewan River, Canada, and part of the landslide was buried by continued deposition. The rate of alluvial deposition was determined by radiocarbon dating to be fairly uniform at about 2.4 mm/year. By measuring the depth of the landslide shear zone below the present surface of the alluvium, an age of about 4000 years b.p. was estimated.

Johnson (1987) discusses some other geomorphic methods to date landslide movement, including correlation of landsliding with specific periods of fluvial downcutting or aggradation and correlation with known limits of ice sheets.

Analysis of soil-profile development also is a potential tool for dating landslides. New soil profiles will begin to develop on disrupted landslide surfaces. If such surfaces can be identified, dating the newly developed soil profile will indicate the age of movement (Small and Clark, 1982;

Birkeland, 1984; Knuepfer, 1988; Birkeland et al., 1991).

## 4. Interpreting an earthquake origin for landslides

Interpreting an earthquake origin for a landslide or group of landslides is by far the most difficult step in the process, and methods and levels of confidence in the resulting interpretation vary widely. Because paleoseismology is a relatively new field of study, analysis of landslides within that field is, in many respects, embryonic. Only a handful of studies have been published to date that explicitly use landslides to identify and date paleo-earthquakes, although several others develop methods that can be applied in paleoseismic investigations. This section summarizes several basic approaches that have been documented to interpret the seismic origin of landslides.

### 4.1. Regional analysis of landslides

Most paleoseismic landslide studies involve analysis of large groups of landslides rather than individual features. The premise of these regional analyses is that a group of landslides of the same age that are scattered across a discrete area probably were triggered by a single event of regional extent. In an active seismic zone, that event commonly is inferred to be an earthquake. Such an interpretation may be justified in areas where landslide types and distribution from historical earthquakes have been documented and can be used as a standard. In areas where such historical observations are absent, assuming an earthquake origin for landslides of synchronous age is much more tenuous, primarily because other regional-scale triggering events, such as large storms, also can trigger widespread landslides having identical ages and spatial distribution.

Crozier (1992) cited six criteria to support a seismic origin for some landslides in New Zealand; these criteria can be applied generally: (1) ongoing seismicity in the region, which has triggered landslides, (2) coincidence of landslide distribution with an active fault or seismic zone, (3) geotechnical slope-stability analyses showing that earth-

quake shaking would have been required to induce slope failure, (4) large size of landslides, (5) presence of liquefaction features associated with the landslides, and (6) landslide distribution that cannot be explained solely on the basis of geological or geomorphic conditions. Obviously, the more of these criteria that are satisfied, the stronger the case for seismic origin.

Russian scientists were the first to analyze the distribution and ages of landslides in seismic zones for paleoseismic analysis. Several papers in Russian deal with the development and application of such studies in Central Asia, but these papers are not readily available outside Russia. A few papers by Russian authors written in English that reference this body of Russian literature are discussed below.

Nikonov (1988) estimated that analysis of landslides in a region can detect earthquakes having magnitudes greater than 6.5 and that epicentral zones can be located within about 10 km. Analysis of fault features is considered preferable for epicentral location and magnitude estimates; analysis of landslides is preferable for age determination (Nikonov, 1988). The method developed by the Russians (Nikonov, 1988) involves complementary studies of fault-related features and shaking-induced features in a known seismic zone. The premise of the approach is that large earthquakes in mountainous areas trigger many landslides, and that the number, size, and areal extent of the landslides are proportional to the size of the earthquake (Solonenko, 1977). Many landslides in a seismic zone are dated either by radiocarbon or lichenometry; if one or more groups of landslides cluster in both space and time, then an earthquake origin is inferred (Nikonov, 1988). Each age cluster is interpreted to define a different paleo-earthquake. Generally, no criteria other than synchronous age are used, so the seismic origin of these landslides is, to a great degree, simply assumed. An earthquake origin is more certain in cases where landslide ages match ages of local fault features and where the types of landslides correspond to those documented in previous earthquakes (Solonenko, 1977). Based on historical observations that large, deep-seated landslides are triggered only within Modified Mercalli Intensity

(MMI) isoseismals VII–IX, only large earthquakes that triggered large, well-preserved landslides have been interpreted from such landslide studies (Nikonov, 1988). This method was applied to rock-avalanche deposits in the epicentral region of the 1907 Karatog and 1949 Khait earthquakes (both $M \approx 7.4$) in Tadjikistan (Nikonov and Shebalina, 1979). Lichenometric ages from young-looking deposits near the epicenter of these two earthquakes correlate with the 1907 and 1949 earthquakes, respectively. Lichenometric dates from the older parts of the deposits suggest an earlier earthquake about 200 years before the study.

Tibaldi et al. (1995) analyzed the distribution of landslides triggered by the 1987 Ecuador earthquakes ($M = 6.9, 6.1$) and compared this distribution with locations of known faults and recent earthquake epicenters. They found good correlation between the elongation of the landslide distribution and the location and dimensions of the seismogenic faults in the area; thus, they concluded that this method could be used to reconstruct the geometry of seismogenic faults in other areas where synchronous landslide distributions can be mapped.

Lichenometry has been used to date rock-fall deposits and rock-fall scarps near the Hope fault (Bull et al., 1991) and the Alpine fault (Bull, 1996) in New Zealand. Recent ages of deposits were linked to historical earthquakes, and older deposits were interpreted to have been triggered by previous earthquakes.

Adams (1981a) used landslide-dammed lakes in New Zealand to identify paleo-earthquakes. He examined 17 historical landslide-dammed lakes and found that 15 of them formed during earthquakes; he therefore concluded that a seismic origin reasonably can be inferred if several synchronous prehistoric landslide dams cluster in an area. Perrin and Hancox (1992) later confirmed that most landslide dams in parts of New Zealand were, indeed, seismically triggered. Adams (1981a) estimated magnitudes of prehistoric earthquakes by comparing the areal extents of landslide dams of a given age with areal extents of landslide dams in historical earthquakes. He dated a group of prehistoric landslide-dammed lakes on South

Island, New Zealand, using three types of samples: (1) woody detritus in the debris of the landslide dams, (2) standing trees drowned by the lakes, and (3) submerged soil horizons cored beneath lake sediment. His results indicate an earthquake of magnitude 7.4 in about A.D. 1650. Adams (1981a) indicated that such analyses could identify earthquakes of $M \geq 6.75$ that occurred within the past few hundred or thousand years.

Schuster et al. (1992) used a similar approach to date prehistoric rock avalanches that dammed streams in the Olympic Mountains in the State of Washington. Synchronous dates for several such avalanches indicate a common triggering event at about 1100 years b.p., which they argued was a large earthquake. Several lines of evidence for seismic triggering were cited: (1) the rock that failed is not known to have failed historically either during large storms or in moderate earthquakes; (2) more than 40% of a recent inventory of worldwide rock avalanches that formed landslide dams were formed by earthquake shaking (Costa and Schuster, 1991); and (3) in New Zealand, the distribution of landslide-dammed lakes approximates the distribution of shallow earthquakes having magnitudes 6.5 or greater (Perrin and Hancox, 1992).

Jacoby et al. (1992) used dendrochronology to date prehistoric landslides that moved into Lake Washington near Seattle. They were able to correlate the tree-ring records from these landslides directly with a tree buried in a tsunami deposit elsewhere in the region. Thus, they inferred an earthquake origin for the Lake Washington landsliding since it was synchronous with a deposit of more certain seismic origin.

Jibson and Keefer (1989) used a regional analysis based on both spatial distribution and synchronous age. They used discriminant analysis and multivariate regression to analyze the geographic distribution of three distinct types of landslides along bluffs that extend more than 300 km through the New Madrid seismic zone. Field evidence indicated that landslides of two of the three types (old coherent slides and earth flows) were synchronous and could have ages consistent with triggering in the 1811–12 earthquakes there; landslides of the third type (young rotational slumps)

appeared much younger and unrelated to seismic activity. The bluffs were divided into segments 762 m (2500 ft) long, and the percentage of the length of each segment covered by landslides of the three types was measured for use as the dependent variable in the statistical analyses. Independent variables measured for each segment included slope height, slope angle, stratigraphic thicknesses of various units, slope aspect, and proximity to the estimated hypocenters of the 1811–12 New Madrid earthquakes. Discriminant analysis showed that bluffs having old coherent slides and earth flows are significantly closer to the estimated hypocenters of the 1811–12 earthquakes than bluffs without these types of slides (Jibson and Keefer, 1989). Bluffs having young slumps showed no such correlation. Multiple regression analysis, which simultaneously combined all factors, showed that the distribution of old coherent slides and earth flows correlates strongly with proximity to the hypocenters of the 1811–12 earthquakes, as well as with slope height and aspect (Jibson and Keefer, 1989). Again, young slumps showed no such correlation with earthquake-related independent variables. The results of these statistical analyses thus showed that old coherent slides and earth flows in the New Madrid seismic zone are spatially related to the 1811–12 earthquake hypocenters and thus probably formed in those earthquakes. This type of analysis can be used only in areas where landslide locations can be correlated with well-defined seismic source zones.

## 4.2. Submarine landslides and turbidites

The classic paper by Heezen and Ewing (1952) demonstrated that large offshore earthquakes can trigger huge turbidity currents having regional extent. They described the Grand Banks turbidity current, which was triggered in the epicentral area of a magnitude 7.2 earthquake on 28 November 1929. The Grand Banks turbidity current involved detachment and downslope movement of submarine sediment along 240 km of the continental shelf; after traveling 650 km from its source, the turbidity current still was moving faster than 20 km/h and therefore probably continued to move for additional hundreds of kilometers. Heezen and

Ewing (1952) postulated that the earthquake triggered submarine slumps along an extensive length of the continental shelf corresponding to the epicentral zone of the earthquake and that these slumps transformed into turbidity currents that moved as rapidly as 100 km/h down slopes averaging only about 1.5°.

More recently, several studies have confirmed the triggering of large submarine landslides and turbidity currents by earthquakes. Perissoratis et al. (1984) documented a slump covering 15–20 km$^2$ in the eastern Korintiakos Gulf along the coast of Greece triggered by a series of earthquakes ($M = 6.4$–6.7) from 24 February to 4 March 1981. Field et al. (1982) documented a sediment flow/lateral spread on a 0.25° slope on the submarine Klamath River delta off the coast of northern California; the feature extends along 20 km of the delta front and is about 1 km long (from scarp to toe). The very low slope and the presence of liquefaction features on the surface both suggest seismic triggering, and repeated bottom surveys before and after the $M = 6.5$–7.2 offshore earthquake of 8 November 1980, conclusively linked the landslide to the earthquake. Lee and Edwards (1986) analyzed the stability of four submarine landslides off the coasts of California and Alaska and concluded that three of them required seismic shaking to have triggered failure. These studies provide the basis for interpreting older submarine landslides and turbidite deposits in terms of seismic triggering.

Several investigators have studied turbidites for paleoseismic interpretation. Kastens (1984) studied submarine debris flows and turbidites from the Calabrian Ridge off the coast of Italy and was able to temporally correlate deposits across several basins. This correlation is inconsistent with a mechanism of gradual oversteepening and slope failure from long-term sedimentation, which would produce temporally independent deposits in different basins. Thus, a seismic origin is postulated because of regional extent and proximity to the seismically active Aegean and Appenine–Sicily arcs. Kastens (1984) identified four debris-flow/turbidite events between 8000 and 14 000 years b.p. and thus estimated a 1500-year recurrence interval between postulated seismic trigger-

ing events during that period. She also compared estimates of peak ground accelerations having return periods of 1500 years in the region with estimated ground accelerations required to trigger the submarine debris flows to show that seismic triggering is a reasonable interpretation.

Adams (1990) conducted a similar study along the Cascadia subduction zone off the coast of Washington and Oregon. He collected bottom core samples over a broad region and documented deposits from 13 turbidity currents having regional extent. He postulated triggering by very large earthquakes because each of these deposits originated in multiple independent channels 50–150 km apart and merged to form one large turbidity current. Synchronous, independent triggering by local endogenic processes (such as local oversteepening from long-term sedimentation) is highly unlikely. The relatively regular time interval between deposits likewise implies triggering by earthquakes having regular recurrence intervals. The mean recurrence interval between the 13 turbidites was $590 \pm 50$ years, and the very broad regional extent suggests triggering earthquakes in the magnitude-9 range. Using current sedimentation rates, Adams (1990) argued that the most recent turbidite likely occurred about 300 years b.p., which agrees with independent paleoseismic evidence of a great Cascadia earthquake at about that time (Atwater, 1987).

Analysis of turbidites also provides an opportunity to make paleoseismic interpretations much further back in the geological record. Mutti et al. (1984) studied Cretaceous and Tertiary flysch sequences in Italy for paleoseismic interpretation. They used the term "seismoturbidite" for turbidites interpreted as being triggered by earthquake shaking. Primary criteria for this interpretation include (1) exceptional volumes ($\sim 100$ km$^3$) and thicknesses ($\geq 100$ m) that are 1–2 orders of magnitude greater than the largest "normal" turbidites in the region; (2) basinwide extent of distinct, synchronous, sheet-like deposits that are easily mappable over large areas; (3) lack of vertical and lateral facies associations with long-lived channel-lobe turbidite systems; and (4) proximity to seismic source zones. Additional criteria include irregular vertical spacing (indicating erratic occurrence),

ages and repeat times proportional to the volume of the deposit, and inability to explain the deposits in terms of meteorological or eustatic processes. Using these criteria, Mutti et al. (1984) interpreted repeat intervals for large earthquakes triggering seismoturbidites in ancient rock sequences: an Upper Cretaceous sequence yielded repeat times of about 200 000 years, an Eocene sequence repeat times of 500 000–1 000 000 years, and a Miocene sequence repeat times of 2000–45 000 years. Obviously, such interpretations are of little use for modern seismic hazard assessment, but they do provide potentially useful tools for reconstructing the paleoseismic history of a region.

Seguret et al. (1984) used a similar approach to interpret Eocene turbidite sequences of the South Pyrenean basin in Spain. They used the term "megaturbidite" in the same sense as seismoturbidite was defined above. Using diagnostic criteria similar to those of Mutti et al. (1984), they interpreted several megaturbidite deposits to have been seismically triggered. Based on the size and regional extent of these deposits, they postulated triggering earthquakes having magnitudes of 7.0–7.5. Average recurrence intervals for these Eocene events is about 500 000 years.

## 4.3. Landslide morphology

Some landslides have morphologies that strongly suggest triggering by earthquake shaking. For example, stability analyses of landslides on low-angle basal shear surfaces show that they generally form much more readily under the influence of earthquake shaking than in other conditions (Hansen, 1965; Jibson and Keefer, 1988, 1993). Landslides that formed as a result of liquefaction of subsurface layers also are much more likely to have formed seismically than aseismically (Seed, 1968). Perrin and Hancox (1992) indicated that slides that form as a result of intense rainfall are more fluid and tend to spread out more across a depositional area, whereas seismically induced landslides may have a blockier appearance and a more limited depositional extent in some cases. None of these criteria are definitive, but the types and characteristics of landslides described above

do suggest seismic triggering and can be used as corroborative evidence of earthquake triggering.

Solonenko (1977) described several types of earthquake-triggered landslides documented in the former Soviet Union, some of which have morphologies that he argued may be unique to seismic origin. His descriptions of such landslides can be condensed into six types: (1) subsidence of areas tens of square kilometers in extent by the opening of fracture systems in very large ($M>8$) earthquakes; (2) collapse of slopes and mountain spurs crossed by active faults; (3) toppling of steep mountain peaks; (4) translational or rotational sliding of topographic benches covering several square kilometers; (5) rock falls and rock avalanches having abnormally long runout distances, including extreme runout events that may have moved on an air cushion; and (6) "ground avalanches and flows," where thick deposits of weak sediment such as loess collapse and flow large distances even on nearly level ground.

Landslide size also is cited widely as evidence of seismic triggering (e.g., Whitehouse and Griffiths, 1983; Nikonov, 1988; Crozier, 1992). In the case of turbidites, large size is a definitive factor because of the criteria of multiple, independently triggered sources over a large area. For terrestrial landslides, use of size to demonstrate seismic origin is more tenuous. Size commonly is inferred to be a factor because of observations of large landslides in past earthquakes (Solonenko, 1977; Whitehouse and Griffiths, 1983; Nikonov, 1988). In areas where large landslides have been documented in historical time to occur only during earthquakes, large size of prehistoric landslides may suggest seismic origin and may even be used to infer the relative size of the triggering earthquake (Nikonov, 1988). It must be remembered, however, that landslides of all sizes form in the absence of earthquake shaking in a wide variety of environments. And Naumann and Savigny (1992) reached an opposite conclusion from their analysis of the stability of several rock avalanches in British Columbia, Canada. They showed that the larger slides analyzed were more susceptible to failure from increased pore-water pressure than from earthquake shaking and that earthquakes are more likely to trigger smaller rock falls (Naumann and Savigny, 1992).

A curious but well-documented phenomenon is the activation (or reactivation) of landslides several days after earthquakes. Jibson et al. (1994) list six known instances of such activity: three involved slow-moving earth flows, and three involved fast-moving debris slides/debris flows. The three earth flows – the Kirkwood earth flow, following the 1959 $M$-7.1 Hebgen Lake, Montana, earthquake (Hadley et al., 1983), and the Chordi and Zhashkva landslides, following the 1991 $M_S$-7.0 Racha, Republic of Georgia, earthquake (Jibson et al., 1994) – were similar in size (250–500 m wide, 1000 m long), began moving 3–5 days after the earthquakes, and moved 30–70 m in the 3–4 weeks following the earthquakes. Large (0.2–2.5 $\times 10^6$ m$^3$) debris slides/debris flows occurred 13 days after the 1906 $M$-8.25 San Francisco, California earthquake; 3 days after the 1949 $M_b$ 7.1 Tacoma, Washington earthquake; and 2 days after the 1983 $M$-7.3 Borah Peak, Idaho, earthquake (Jibson et al., 1994). Several investigators (e.g., Keefer et al., 1985; Wood, 1985; Rojstaczer and Wolf, 1992) have speculated that delayed landslide movement is caused by increased ground-water flow arising from either locally increased permeability or increased pore pressure. The length of the delay may represent the time needed for rising ground-water levels in the slide (or pore pressures on the slide plane) to lower the factor of safety below 1.0. However, because these slides are initiated by ground-water changes that could just as well have been induced nonseismically over a longer period of time, they are not unambiguous indicators of paleoseismicity.

In summary, landslide morphology and size can, in some circumstances, be used as corroborative evidence for seismic triggering, but only when a clear link between a specific morphology or size and earthquake triggering is observed.

## 4.4. Sackungen

Several different interpretations of the origin of sackungen have been proposed. Clearly, topography controls the ridge-parallel geometry of sackungen, and gravity is the principal driving force. But whether initiation of movement is by long-term creep, faulting, strong shaking, or a combina-

tion of factors has been debated. Bovis (1982) and Varnes et al. (1989), who studied sackungen in western North America, argued that movement stems from long-term, gravity-driven creep, although both studies mention tectonism as a possible contributor in some cases. On the other hand, Beck's investigations (Beck, 1968) of sackungen in New Zealand concluded that earthquake shaking was the most likely trigger of movement, primarily because the sackung topography appeared stable over long periods of seismic quiescence and because sackungen were abundant in seismically active areas there. Jahn (1964) likewise surmised that sackungen in the Tatra Mountains of Czechoslovakia were triggered by earthquakes. Tabor (1971) indicated that earthquake shaking might play a minor role in sackung formation in the Olympic Mountains of Washington. Using sackungen for paleoseismic analysis appears tenuous, at best, and requires independent evidence of seismic triggering. To date, no criteria for establishing the seismic origin of sackungen have been published.

## 4.5. Interpretation of sedimentary structures

Some sedimentary structures have been interpreted as being seismically generated and thus could be used for paleoseismic interpretation. Although such structures (commonly called *seismites*) are not landslides, they do involve seismic disturbance of surficial earth material. Among the first such studies was that by Seilacher (1969), in which he describes "fault-graded" bedding and argues that seismic shaking is the most likely origin of this type of structure. Fault-graded bedding consists of a sequence, perhaps several decimeters thick, that includes (from top down) (1) a liquefied zone, (2) a rubble zone, and (3) a step-faulted zone, all in gradational contact. His observation of three such sequences in a 10-m-thick section of Miocene Monterey Shale in coastal California led him to conclude that such structures result from very rare, very strong earthquakes. A subsequent study (Seilacher, 1984) identified pleated lamination, convex-down stacking of bowl-shaped shells, and current orientation in starved shell ripples as addi-

tional sedimentary structures that may have seismic origin.

Spalletta and Vai (1984) examined Upper Devonian turbidites in the Carnic region of northern Italy and interpreted a seismic origin on the basis of sedimentological structures as well as the geometries of the deposits. Their diagnostic sedimentological criteria for seismic triggering is the presence of "intraclast parabreccias," described as being caused by "shallow earthquakes generat(ing) in situ (autoclastic) brecciation of the early lithified, centimeters-thick, surficial pelagic carbonate layer" (Spalletta and Vai, 1984, pp. 135). This brecciation is followed within seconds to hours by a sandy turbidity current triggered upslope by the same earthquake. Repeated sections containing such structures were discovered, but no recurrence intervals were estimated.

Several other such studies have interpreted various types of soft-sediment deformation features as being seismically induced and have drawn tentative conclusions about the paleoseismic history of different regions (El-Isa and Mustafa, 1986; Plaziat et al., 1990; Pratt, 1992, 1994). And in an interesting attempt to model the effects of seismicity on sedimentary basins, Allen (1986) combined empirical equations describing earthquake-magnitude recurrence intervals and maximum distances at which liquefaction-induced ground failure can occur for a given earthquake magnitude to model the potential frequency and spatial distribution of earthquake-triggered sediment deformation in sedimentary basins.

Large rock avalanches commonly are triggered by large earthquakes (Keefer, 1984). Sedimentological criteria for identifying rock-avalanche deposits in the geological record have been developed (Yarnold and Lombard, 1989) and could potentially be applied to paleoseismic studies if diagnostic criteria for seismic triggering were developed.

Studies of in-place deformation of lake-bottom sediment by seismically induced liquefaction have identified criteria by which lacustrine sedimentary structures can be attributed to earthquake shaking (Sims, 1973, 1975; Hempton and Dewey, 1983). Such liquefaction structures are discussed in Obermeier's paper in this volume.

## 4.6. Lacustrine sediment pulses caused by landslides

Adams (1980) measured sediment loads of rivers in New Zealand immediately following earthquakes and observed an order-of-magnitude increase in load for a period of several months. He correlated increases in load in different areas with the density of earthquake-triggered landslides in those areas and concluded that seismically induced landslides cause large increases in fluvial sediment load, which, in turn, cause increases in sedimentation rates in lakes and oceans. These observations have been corroborated with published observations from earthquakes elsewhere (Adams, 1981b).

On the premise of these observations, Doig (1986) analyzed organic-free silt layers 0.3–2.0 cm thick in otherwise organic-rich lake sediment in eastern Canada. Using sedimentation rates and radiometric methods, three of these layers were correlated with known earthquakes of A.D. 1663, 1791, and 1860+1870 (two events combined). Two older silt layers were likewise dated and attributed to paleo-earthquakes in A.D. 1060 and 600. Doig (1986) stated that cores from deep lakes likely will yield the best cores for this type of analysis because of lack of bioturbation. He also warned that dating young (a few hundred years) silt layers characterized by lack of organic material can be difficult; he suggested that lead-210 and cesium-137 are the ideal radiometric methods for this type of analysis.

## 4.7. Landslides that straddle faults

In some areas, landslides have formed on slopes immediately above fault traces, and the slide mass has extended across the trace (Hunt, 1975; Morton and Sadler, 1989). Subsequent surface movement of such a fault would offset the landslide mass and allow estimation of fault slip rates if the slide could be dated. This approach does not require that the landslide be seismically triggered, because the paleoseismic interpretation is based on post-land-slide fault offset of the landslide mass. However, landslides triggered in the immediate vicinity of active faults commonly are seismically triggered (Burrows, 1975).

## 4.8. Precariously balanced rocks

Brune (1996) used precariously balanced rocks as crude paleoseismoscopes. He used field observations supplemented by theoretical modeling, numerical simulation, and physical modeling to estimate threshold accelerations needed to topple various configurations of balanced rocks. In general, horizontal accelerations of about 0.1–0.3 $g$ were found to be needed to topple most configurations studied. Brune studied several areas around epicenters of historical earthquakes and found few or no precariously balanced rocks; he concluded that such rocks had been toppled by previous earthquakes. He also investigated areas of unknown seismic potential and concluded that those areas where balanced rocks were present had not experienced ground shaking exceeding about 0.1–0.2 $g$ in the past several hundred or thousand years, the estimated time needed to form the balanced rocks. Although this approach is still being developed, it may prove useful in determining if an area has experienced a certain threshold level of ground shaking in the past few thousand years.

## 4.9. Speleothems

Forti and Postpischl (1984) detailed a method for analyzing the toppling of stalagmites for paleoseismic interpretation. By measuring and dating tilting and collapse of many stalagmites in a region, they differentiated sudden (seismic) versus gradual movements and local versus regional causes. Tilting and collapse events are dated by analysis of radiometrically determined speleothem growth rates, which allows interpretation for about the last 100 000 years. Because stalagmites are inverted pendulums, the minimum ground shaking necessary to cause collapse can be estimated fairly easily by pseudostatic engineering analysis. Although the method has some promise, it has not, thus far, been applied successfully to identify and date specific paleo-earthquakes.

## 4.10. Summary

Several methods for interpreting the seismic origin of landslides have been developed and, in some cases, successfully applied to paleoseismic analysis. Virtually all of the methods summarized in this section have one aspect in common, which is stated explicitly in most papers: the seismic origin of the features being interpreted remains tentative and cannot be proven, because in each case a nonseismic process could have produced the observed features. Circumstantial evidence for seismic triggering ranges from very strong to extremely tenuous. Indeed, on the latter end of the spectrum, the reasoning can be rather circular: an earthquake origin for a feature is assumed and then an earthquake origin is interpreted and concluded from analysis of that feature. Any paleoseismic interpretation of a feature is limited primarily by the certainty with which seismic triggering can be established. The following section addresses this dilemma by describing an approach to directly assess the conditions leading to failure of individual landslides.

## 5. Analysis of the seismic origin of a landslide

The most direct way to assess the relative likelihood of seismic versus aseismic triggering of an individual landslide is to apply established methods of static and dynamic slope-stability analysis (Lee and Edwards, 1986; Crozier, 1992; Jibson and Keefer, 1993). The first step in such an analysis involves constructing a detailed slope-stability model of static conditions to determine if failure is likely to have occurred in any reasonable set of ground-water and shear-strength conditions in the absence of earthquake shaking. All potential nonseismic factors must be considered; these might include processes such as fluvial or coastal erosion that oversteepens the slope or undrained failure resulting from rapid drawdown (for slopes subject to submersion). If aseismic failure can reasonably be excluded even in worst-case conditions (minimum shear strength, maximum piezometric head), then an earthquake origin can be inferred. Dynamic slope-stability analyses can then be used

to estimate the minimum shaking conditions that would have been required to cause failure. In the sections that follow, a method for conducting such an analysis is described using an example from the New Madrid seismic zone summarized from Jibson and Keefer (1993).

## 5.1. Physical setting of landslides in the New Madrid seismic zone

The New Madrid earthquakes of 1811–12 (Fuller, 1912) triggered many large landslides along the bluffs that form the eastern edge of the Mississippi River alluvial plain in Tennessee and Kentucky (Fig. 1). Many landslide features currently are visible along these bluffs, and one of these landslides is analyzed below to determine if a seismic versus nonseismic origin can be established with a reasonable level of confidence.

The bluffs in the study area are not, for the most part, active river banks and thus are subject to landsliding from fluvial erosion in only a few locations. The bluffs stand as high as 70 m above the alluvial plain of the Mississippi River and therefore are not subject to landsliding from conditions such as rapid drawdown because the bluff is never inundated by flooding to a significant height. The average height of the bluffs in this area is 35 m, and slope angles range from a few degrees to almost vertical, but typically are 15–25°.

The base of the bluffs throughout most of the area is formed by as much as 45 m of shallow-marine clays and silts of the Eocene Jackson Formation (Conrad, 1856). Lying unconformably on the Jackson Formation is as much as 20 m of Pliocene alluvial gravel and sand of the Lafayette Gravel (McGee, 1891; Potter, 1955). The bluffs are capped by 5–50 m of Pleistocene loess lying unconformably on the Jackson Formation and Lafayette Gravel. The average thickness of the loess in the area is about 15 m.

A translational block slide about 11 km north of Dyersburg, TN, referred to as the Stewart landslide, was chosen for detailed analysis (Fig. 1). This landslide is representative of coherent block slides in the area, which previous research (Jibson and Keefer, 1988, 1989) indicated were probably triggered by the 1811–12 earthquakes. Fig. 2 shows
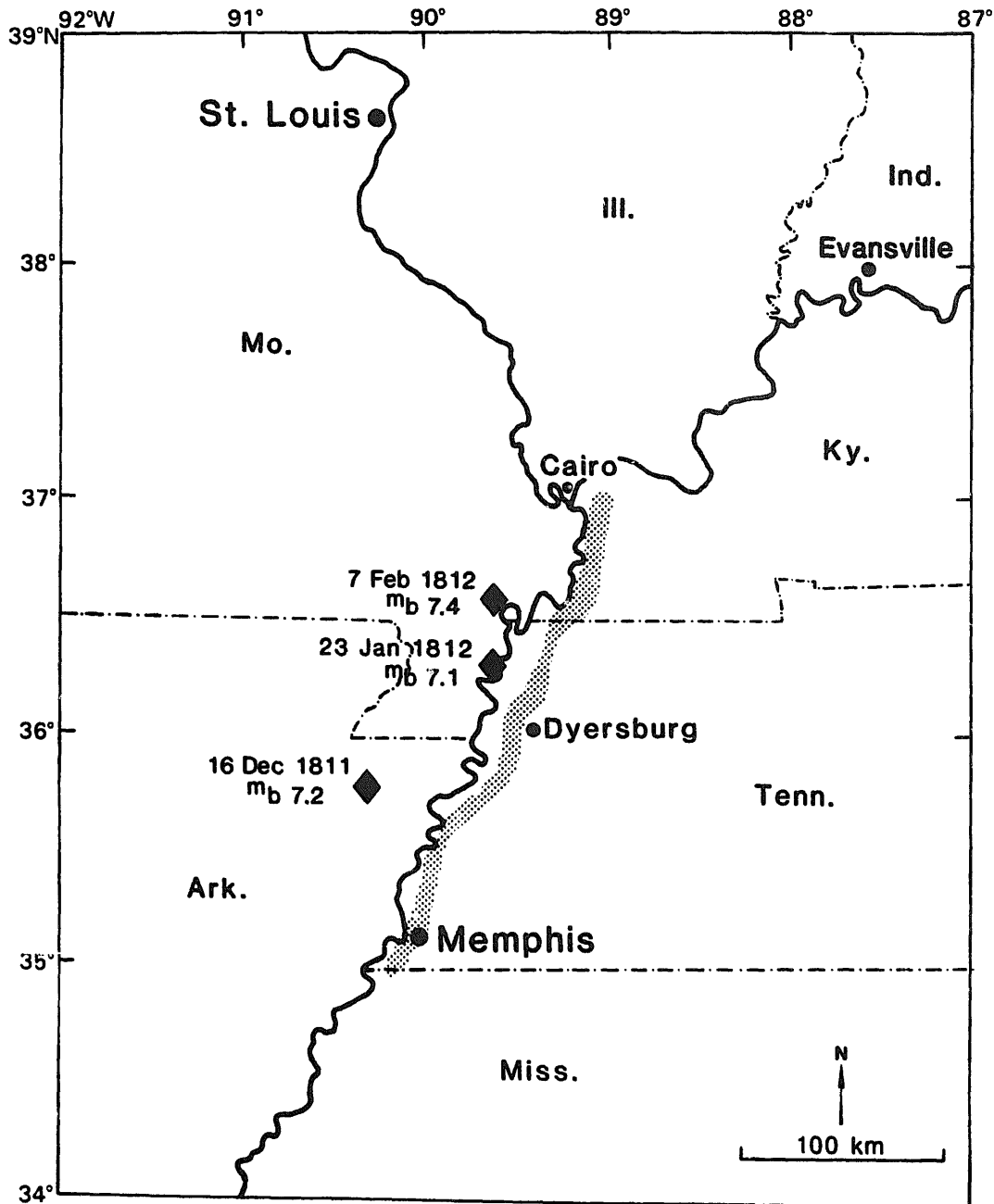
Fig. 1. Map showing estimated epicenters (diamonds), dates, and body-wave magnitudes ($m_b$) of the three largest earthquakes in the 1811–12 New Madrid sequence (from Nuttli, 1973); bluffs (shaded) containing landslides triggered in 1811–12; and the location of the Stewart landslide.

a profile of the Stewart slide; subsurface data is from drilling along the line of profile.

## 5.2. Geotechnical investigation

Four rotary drill holes were placed along the line of profile to determine the bluff stratigraphy

and to procure soil samples for geotechnical testing (Fig. 2). Standard-Penetration testing (SPT) yielded split-spoon samples, which typically were heavily disturbed by the sampling process and were used primarily for determining index properties, such as grain size, plasticity, water content, and color. Several 13-cm-diameter undisturbed
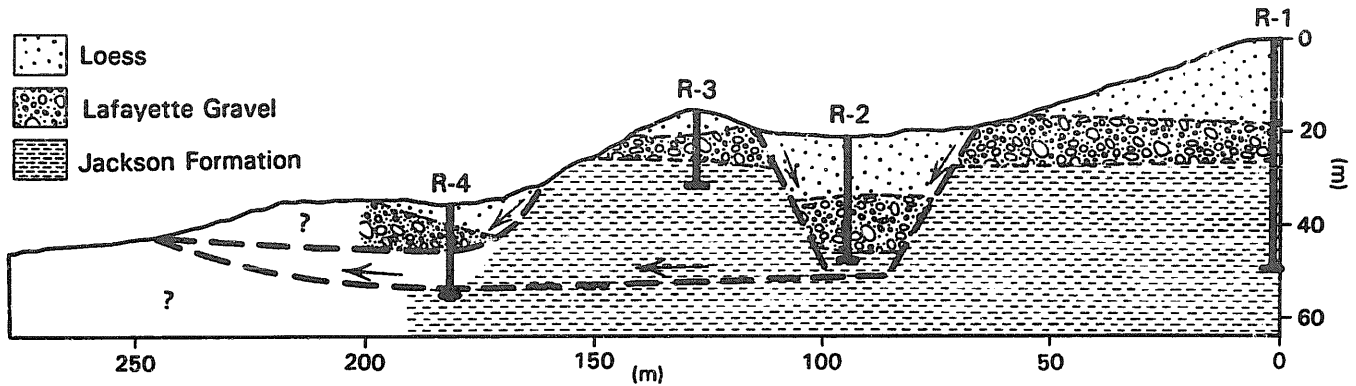
Fig. 2. Cross-section of Stewart landslide showing subsurface stratigraphy (identified from drill holes designated R-1 through R-4) and diagrammatic representation of failure surfaces (heavy dashed lines). Undisturbed stratigraphy is shown at R-1.

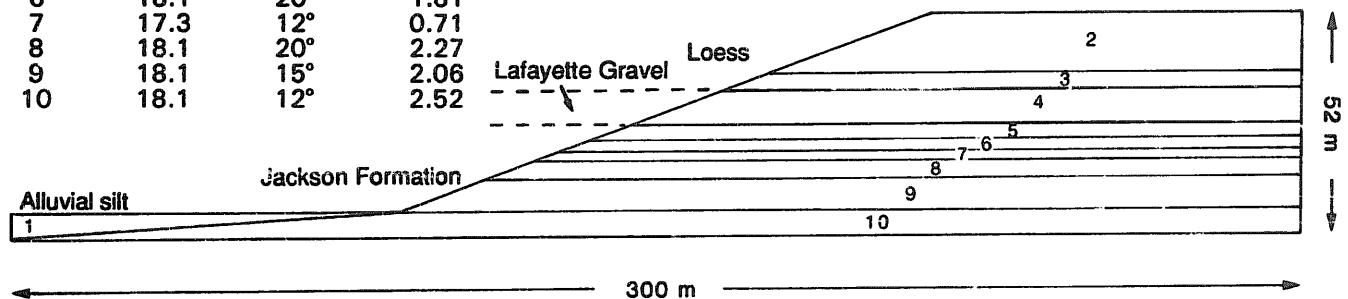| Layer | Unit Weight ($kN/m^3$) | Drained Friction Angle | Drained Cohesion (kPa) |
|---|---|---|---|
| 1 | 19.3 | 34° | 0.25 |
| 2 | 19.6 | 35° | 0.50 |
| 3 | 19.8 | 30° | 0.43 |
| 4 | 22.0 | 32° | 0.32 |
| 5 | 18.1 | 15° | 2.06 |
| 6 | 18.1 | 20° | 1.81 |
| 7 | 17.3 | 12° | 0.71 |
| 8 | 18.1 | 20° | 2.27 |
| 9 | 18.1 | 15° | 2.06 |
| 10 | 18.1 | 12° | 2.52 |



Fig. 3. Idealized model of pre-landslide bluff at Stewart site in drained conditions. Soil properties are shown for each designated layer in the computer model.

piston cores were procured to measure soil unit weight and shear strength, both needed for limit-equilibrium stability analysis. Jibson (1985) described the sampling methods in detail.

Drained shear strengths, for use in static stability analyses, were measured using two methods: (1) direct shear in which the rate of strain was slow enough to allow full drainage and (2) consolidated-undrained triaxial (CUTX) shear in which pore pressures were measured to allow modeling of drained conditions (Jibson, 1985). Undrained shear strengths, for use in dynamic analysis, were measured primarily by CUTX tests. CUTX test results were supplemented by vane-shear and pene-

trometer data and correlation with SPT blow counts where undisturbed samples were unavailable.

### 5.3. Static (aseismic) slope-stability analysis

Fig. 3 shows an idealized model of the pre-landslide bluff in drained conditions, appropriate for modeling static (aseismic) stability. The bluff is 45 m high as measured from the profile (Fig. 2). Undisturbed bluffs adjacent to the Stewart slide have slopes of about 20° and have simple, uniformly sloping faces. Geotechnical properties of the stratigraphic layers in the model were assigned
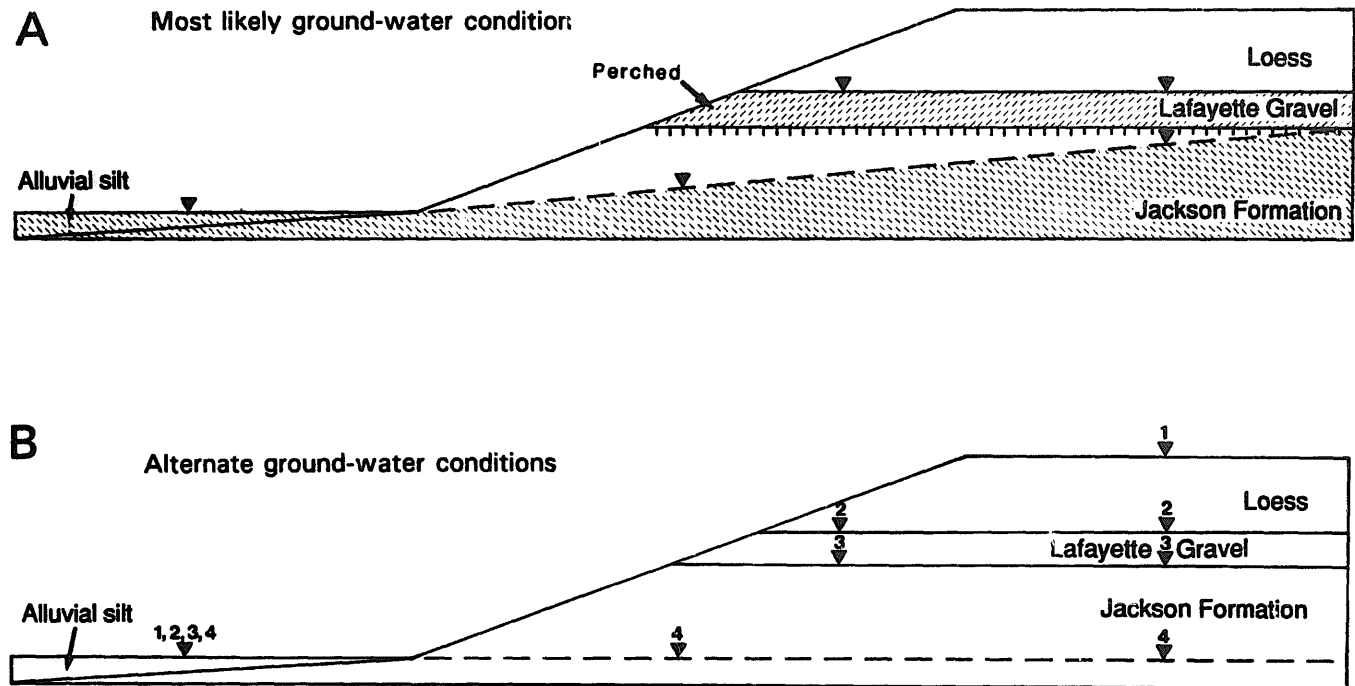
Fig. 4. Ground-water conditions modeled in the slope-stability analyses. (A) Most likely ground-water condition; saturated zones are shown by cross-hatched pattern. (B) Piezometric surfaces of four alternate ground-water conditions are shown by inverted triangles numbered 1–4.

using the results of the shear-strength tests; layers where no shear-strength tests were performed were assigned strengths based on stratigraphic and index-property correlation with layers where strengths were measured (Jibson, 1985).

Lack of published data made modeling ground-water conditions along the bluffs difficult. Therefore, several potential ground-water conditions were modeled (Fig. 4) that effectively bracket the most and least critical conditions that are physically possible. Because of the local topography and hydraulic properties of the bluff materials, the most critical condition modeled (Fig. 4, condition 1) is a more critical situation than can realistically exist in the bluffs and thus provides a worst-case bounding condition. The most likely ground-water condition also was modeled: a water table sloping upward from the base of the bluffs to the top of the Jackson Formation, and a second water table perched on the relatively impermeable Jackson that saturates the Lafayette Gravel.

The STABL computer program (Siegel, 1978) was used to determine the stability of the modeled bluff in aseismic conditions. STABL searches for

the most critical failure surface by randomly generating circular, wedge, and irregular slip surfaces and calculating the factor of safety[1] for each generated surface. The program plots the ten most critical surfaces of each type and their factors of safety. The geometry of the actual failure surface (shown diagrammatically in Fig. 2) was determined by locating weak or disturbed layers by drilling and by analysis of the surface geometry of the landslide. The safety factor for this surface was calculated using the simplified Janbu method (Siegel, 1978) for each ground-water condition.

Determining the stability of the bluffs from the factor of safety requires judgment. Gedney and Weber (1978) recommended that engineered slopes have safety factors between 1.25 and 1.50 for the type of analysis used. Because of the high density of good-quality geotechnical data, this range is

---

[1]The factor of safety (FS) is the ratio of the sum of the resisting forces that act to inhibit slope movement to the sum of the driving forces that tend to cause movement. Slopes having factors of safety greater than 1.0 are thus stable; those having factors of safety less than 1.0 should move.

Table 2
Static factors of safety from stability analyses of the Stewart landslide in drained and undrained conditions

| Type of failure surface | Location of piezometric surface: | | | | |
|---|---|---|---|---|---|
| | Base of bluff[a] | Top of Jackson[b] Formation | Top of Lafayette[c] Gravel | Top of Bluff[d] | Most Likely[e] |
| Drained stability analyses | | | | | |
| Circular | **1.90** | **1.66** | **1.61** | 1.35 | **1.82** |
| Irregular | 1.95 | 1.69 | 1.64 | **1.32** | 1.87 |
| Wedge, Layer 5 | 4.06 | 3.98 | 3.76 | 2.83 | 4.03 |
| Wedge, Layer 6 | 4.24 | 4.03 | 3.80 | 2.79 | 4.23 |
| Wedge, Layer 7 | 2.46 | 2.28 | 2.14 | 1.47 | 2.45 |
| Wedge, Layer 8 | 3.81 | 3.39 | 3.23 | 2.51 | 3.72 |
| Wedge, Layer 9 | 2.83 | 2.48 | 2.38 | 1.88 | 2.71 |
| Wedge, Layer 10 | 2.40 | 2.10 | 2.03 | 1.68 | 2.25 |
| Actual Surface | 1.96 | 1.73 | 1.67 | 1.40 | 1.88 |
| Undrained stability analyses | | | | | |
| Circular | 1.72 | 1.72 | 1.64 | **1.99** | 1.62 |
| Irregular | **1.64** | **1.64** | **1.55** | 2.16 | **1.53** |
| Wedge, Layer 5 | 2.81 | 2.81 | 2.50 | 3.59 | 2.49 |
| Wedge, Layer 6 | 3.23 | 3.23 | 2.96 | 3.84 | 2.93 |
| Wedge, Layer 7 | 2.19 | 2.19 | 1.99 | 2.81 | 1.97 |
| Wedge, Layer 8 | 3.18 | 3.18 | 3.05 | 3.57 | 3.02 |
| Wedge, Layer 9 | 2.00 | 2.00 | 1.89 | 2.41 | 1.87 |
| Wedge, Layer 10 | 1.99 | 1.99 | 1.88 | 2.25 | 1.87 |
| Actual Surface | 1.74 | 1.74 | 1.66 | 2.12 | 1.65 |

Most critical surface for each ground-water condition shown in bold type.[a]Fig. 4B, piezometric surface 4.[b]Fig. 4B, piezometric surface 3.[c]Fig. 4B, piezometric surface 2.[d]Fig. 4B, piezometric surface 1.[e]Fig. 4A.

used as the criterion to evaluate slope stability: between FS 1.00 and 1.25, slopes are considered to be marginally stable; between FS 1.25 and 1.50, slopes are considered to be stable; and above FS 1.50, slopes are considered to be very stable.

The results of the stability analyses are summarized in Table 2. The lowest factor of safety in the most critical ground-water condition is 1.32, which

indicates that the bluff at the Stewart site is stable in aseismic conditions even in the most critical ground-water condition. In the most likely ground-water condition (sloped and perched), the minimum factor of safety is 1.82, indicating a very stable bluff. The factor of safety of the actual failure surface in the most likely ground-water condition is 1.88.
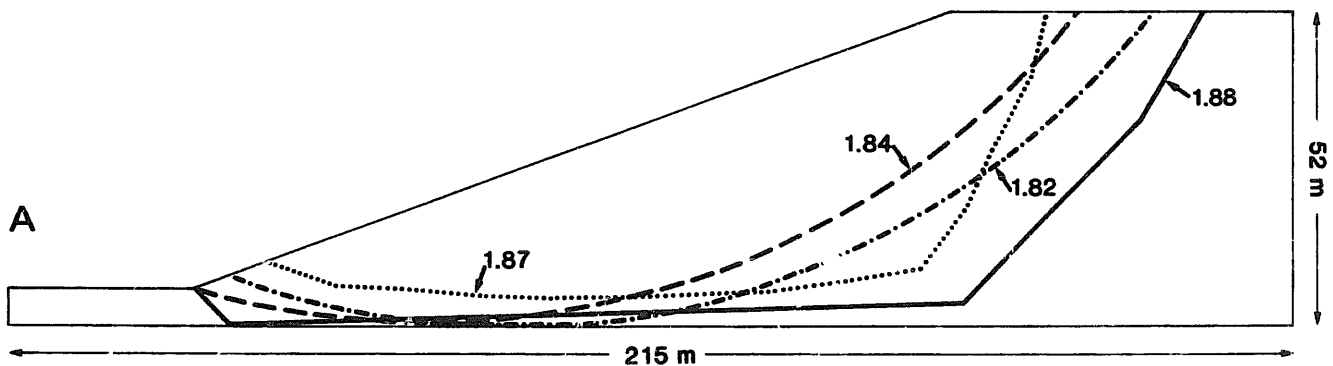


Fig. 5. The three most critical slip surfaces and their factors of safety (FS=1.82, 1.84, 1.87) for static, drained conditions at the Stewart site in the most likely ground-water condition. Heavy, solid line shows estimated location of actual failure surface (FS=1.88).

Our analysis shows that an artesian piezometric surface tens of meters above ground level at the top of the bluff would be needed to reduce the factor of safety to 1.0. Such an artesian condition is impossible because (1) the regional geology and topography preclude such a condition because the top of the bluff is 30–70 m above the alluvial plain, and no topographically higher artesian recharge area exists, and (2) a piezometric surface high above the bluff-top that dips steeply to the base of the bluff is physically unrealistic.

Fig. 5 shows the locations of the most critical slip surfaces of various shapes and of the actual slip surface. All the surfaces have grossly similar shapes, but the most critical computer-generated surfaces all lie well above the actual failure surface. This disparity suggests that the sliding did not take place under drained, static conditions.

The rather high factors of safety, even in unrealistically high ground-water conditions, and the disparity between the most critical computer-generated slip surfaces and the actual surface indicate that it is highly unlikely that the existing landslide at the Stewart site formed in aseismic, drained conditions.

## 5.4. Dynamic (seismic) slope-stability analysis

Jibson and Keefer (1993) used the dynamic displacement analysis developed by Newmark (1965), now used widely in engineering practice (Seed, 1979), to evaluate the seismic stability of the bluff. In the Newmark method a landslide is modeled as a rigid friction block that begins to move when a given critical acceleration is exceeded; critical acceleration is defined as the acceleration required to overcome frictional resistance and initiate sliding on an inclined plane. The analysis calculates the cumulative permanent displacement of the block as it is subjected to the effects of an earthquake acceleration-time (strong-motion) history, and the user judges the significance of the displacement. Laboratory model tests (Goodman and Seed, 1966) and analysis of actual earthquake-induced landslides (Wilson and Keefer, 1983) have confirmed that Newmark's method can fairly accurately predict landslide displacements if slope geometry and soil properties are known accurately

and if earthquake ground accelerations can be estimated using real or artificial acceleration-time histories. I have provided a detailed treatment of how to conduct a Newmark analysis on landslides in natural slopes elsewhere (Jibson, 1993).

Newmark (1965) showed that the critical acceleration is a simple function of the static factor of safety and the landslide geometry; it can be expressed as

$$a_c = (FS - 1)g \sin \alpha, \tag{1}$$

where $a_c$ is the critical acceleration in terms of a ratio to $g$, the acceleration of Earth's gravity; FS is the static factor of safety; and $\alpha$ is the angle from the horizontal (hereafter called the thrust angle) that the center of mass of the potential landslide block first moves.

The algorithm developed by Wilson and Keefer (1983) is used to apply Newmark's method; it consists simply of double-integrating the portions of the selected acceleration-time history that lie above the critical acceleration of the landslide block. This double integration of the acceleration record yields the cumulative permanent displacement of the block.

Conducting a Newmark analysis requires three pieces of information: (1) the static factor of safety and (2) the thrust angle of the potential landslide (both needed to calculate the critical acceleration), and (3) an earthquake acceleration-time history.

### 5.4.1. Static factor of safety

During earthquakes, soils behave in a so-called undrained manner because excess pore pressures induced by the transient ground deformation cannot dissipate during the brief duration of the shaking; therefore, a layered model of the bluff in undrained conditions was constructed (Fig. 6). Undrained shear strength is treated as a single numerical quantity that is represented in the analysis as cohesion, and the friction angle is taken to be zero (Lambe and Whitman, 1969). Undrained shear strengths used in the model (Fig. 6) were measured directly in the laboratory, as described previously. Because undrained strength depends in large part on consolidation stress, layers of roughly similar thickness were constructed that reflect the
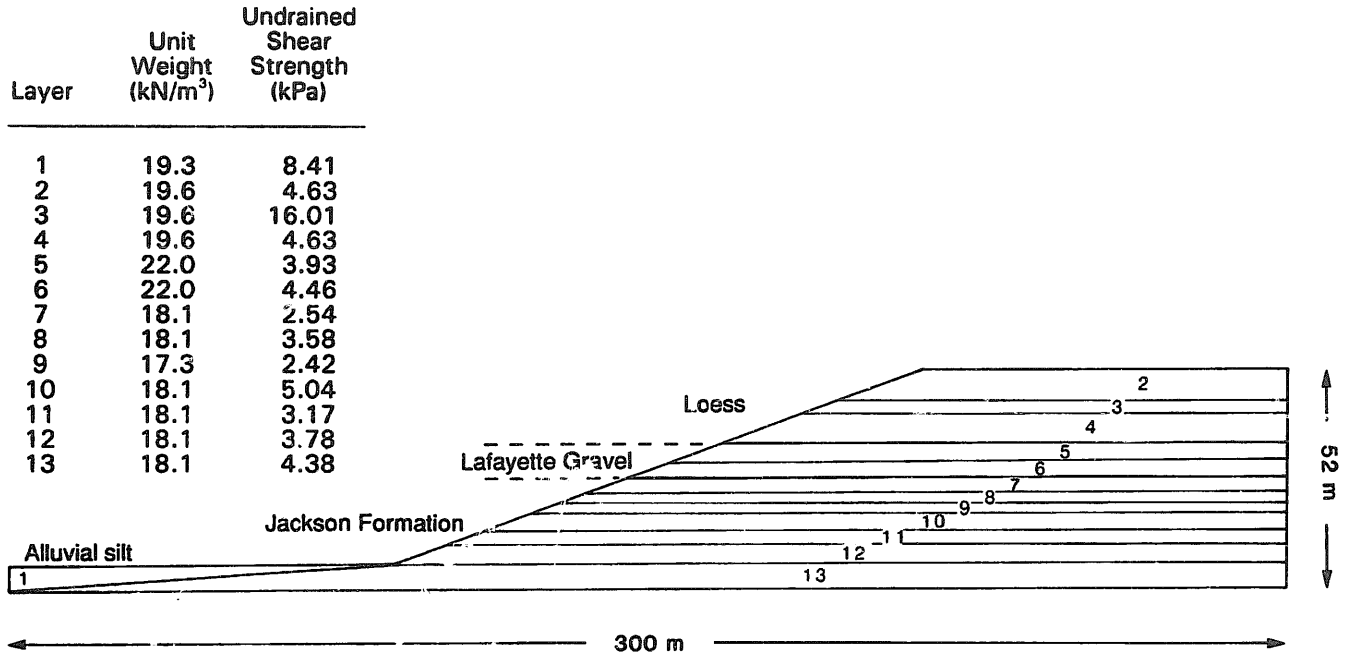
| Layer | Unit Weight (kN/m³) | Undrained Shear Strength (kPa) |
|-------|---------------------|--------------------------------|
| 1 | 19.3 | 8.41 |
| 2 | 19.6 | 4.63 |
| 3 | 19.6 | 16.01 |
| 4 | 19.6 | 4.63 |
| 5 | 22.0 | 3.93 |
| 6 | 22.0 | 4.46 |
| 7 | 18.1 | 2.54 |
| 8 | 18.1 | 3.58 |
| 9 | 17.3 | 2.42 |
| 10 | 18.1 | 5.04 |
| 11 | 18.1 | 3.17 |
| 12 | 18.1 | 3.78 |
| 13 | 18.1 | 4.38 |

Fig. 6. Idealized model of pre-landslide bluff at Stewart site in undrained conditions. Soil properties are shown for each designated layer in the computer model.
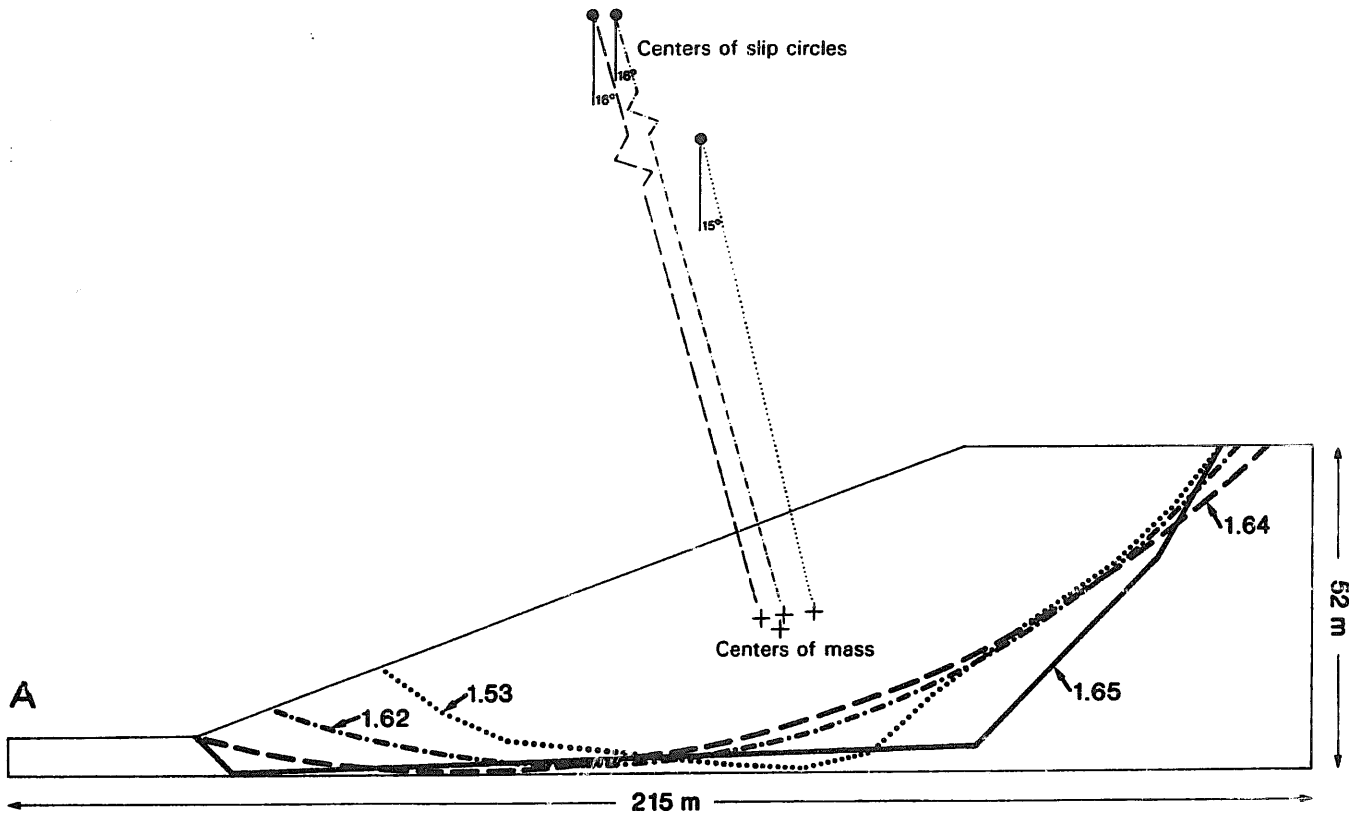
Fig. 7. The three most critical slip surfaces and their factors of safety (FS = 1.53, 1.62, 1.64) for static, undrained conditio is at the Stewart site in the most likely ground-water condition. Heavy, solid line shows estimated location of actual failure surface (FS = 1.65). Geometric construction to determine thrust angle also shown.

increase in shear strength with depth even for relatively homogeneous materials.

STABL was used to generate potential failure surfaces and to determine the most critical failure surface in the same manner as described above for the aseismic stability analysis in drained conditions. Table 2 summarizes the results of the undrained slope stability analyses using this model. The lowest factor of safety is 1.53, which shows that the bluff is statically stable in undrained conditions. Fig. 7 shows the locations of the most critical slip surfaces for the most likely groundwater condition. All the slip surfaces, including the actual failure surface, plot very close to one another and have similar factors of safety. Both circular surfaces have large radii and approximate planar basal shear surfaces, as is expected from the shape of the actual shear surface (Fig. 2). The fact that the most critical computer-generated failure surfaces closely parallel the actual failure surface indicates that the model of the bluffs is reasonable and that slope failure is more likely to have occurred in undrained conditions than in drained conditions.

### 5.4.2. Thrust angle

The thrust angle ($\alpha$) is the direction the center of gravity of the slide mass moves when displacement first occurs. For a planar slip surface parallel to the slope face (an infinite slope), the thrust angle is the slope angle. For rotational movement on a circular surface, Newmark (1965) showed that the thrust angle is the angle between the vertical and a line segment connecting the center of gravity of the landslide mass and the center of the slip circle.

Fig. 7 shows geometric constructions of the thrust angles for the two circular failure surfaces and the circular approximation of the irregular surface. Thrust angles for these surfaces all are 15–16°. The thrust angle of the actual surface is difficult to estimate because of its irregular shape and consequent complex movement. An average inclination of the actual failure surface can be calculated by weighting the inclinations of the line segments forming the actual surface by their relative lengths. This yields an average inclination of 16°, consistent with the other generated surfaces.

### 5.4.3. Earthquake acceleration-time history

The hypothesis being tested is that the Stewart landslide was triggered by the 1811–12 earthquakes; therefore, earthquake acceleration-time histories must be selected to approximate the shaking conditions from the 1811–12 earthquakes at the Stewart site. Choosing strong-motion records to represent the ground motions from the 1811–12 earthquakes is difficult because most available records are from California earthquakes, which probably differ in many respects from large earthquakes in the central United States (e.g., Nuttli, 1983). Differences in the propagation of strong ground motion due to regional differences in attenuation, however, may not be as great as previously believed, and they appear to be significant only at great epicentral distance (>150 km) for very large earthquakes (Hanks and Johnston, 1992). The Stewart site is only 20–70 km from the three estimated epicenters of the 1811–12 earthquakes.

Estimating various ground-motion characteristics of the 1811–12 earthquakes at the Stewart site and comparing these estimated characteristics with those of existing earthquake records provides a basis for choosing an input ground motion. Peak ground acceleration (PGA), duration, and shaking intensity are used for this comparison, and these parameters can be estimated by several methods, as described by Jibson and Keefer (1993). Although PGA is the most commonly used index of strong shaking, it is a rather crude single measure of earthquake shaking intensity because it measures only a single point in an acceleration-time history. A more quantitative measure of total shaking intensity developed by Arias (1970) is useful in seismic hazard analysis and correlates well with distributions of earthquake-induced landslides (Harp and Wilson, 1989, 1995). Arias intensity is the integral over time of the square of the acceleration, expressed as

$$I_a = \pi/2g \int [a(t)]^2 dt, \tag{2}$$

where $I_a$ is the Arias intensity, expressed in units of velocity, and $a(t)$ is the ground acceleration as a function of time. Arias intensity is used as the primary characteristic for comparison in selecting strong-motion records.

Although strong motion has not been recorded for earthquakes in the magnitude range of the

Table 3
Strong-motion records used to model ground shaking from the 1811–12 earthquakes at the Stewart landslide

| Earthquake recording site, component | M | $R$ (km) | $\hat{a}$ ($g$) | $T$ (s) | $I_a$ (m/s) | $D_N$ (cm) |
|---|---|---|---|---|---|---|
| 16 Dec. 1881, New Madrid, MO, Stewart landslide site (estimated) | 8.2 | 68 | 0.39 | 20–40 | 2.7[a], 2.7–5.5[b] | |
| •15 Oct. 1979, Imperial Valley, CA, El Centro differential array, 360° | 6.5 | 7 | 0.49 | 6.6 | 2.1 | 6–8 |
| •24 Nov. 1987, Superstition Hills, CA, Superstition Mountain site 8, 135° | 6.5 | 6 | 0.90 | 12.2 | 6.8 | 23–25 |
| 23 Jan. 1812, New Madrid, MO, Stewart landslide site (estimated) | 8.1 | 24 | 0.74 | 18–40 | 17.4[a], 8.9–19.7[b] | |
| •9 Feb. 1971, San Fernando, CA, Pacoima Dam, 164° | 6.6 | 3 | 1.22 | 6.7 | 9.1 | 50–55 |
| •16 Sept. 1978, Tabas, Iran, 74° | 7.4 | 3 | 0.71 | 16.1 | 10.0 | 39–44 |
| 7 Feb. 1812, New Madrid, MO, Stewart landslide site (estimated) | 8.3 | 44 | 0.71 | 25–40 | 8.2[a], 11.3–18.1[b] | |
| •24 Nov. 1987, Superstition Hills, CA, Superstition Mountain site 8, 135° | 6.5 | 6 | 0.90 | 12.2 | 6.8 | 23–25 |
| •16 Sept. 1978, Tabas, Iran, 74° | 7.4 | 3 | 0.71 | 16.1 | 10.0 | 39–44 |

Characteristics of the 1811–12 earthquakes estimated as described in text. All strong-motion records are from US Geological Survey recording stations except for the Tabas, Iran, record ([Hadley et al., 1983]). M is moment magnitude (estimates for the 1811–12 earthquakes from [Hamilton and Johnston, 1990]); $R$ is earthquake source distance; $\hat{a}$ is peak ground acceleration; $T$ is duration of strong shaking as defined by [Dobry et al. (1978)]; $I_a$ is [Arias (1970)] intensity; $D_N$ is [Newmark (1965)] displacement (range shown covers range of critical accelerations discussed in text). [a]Estimated using Eq. (4) of [Jibson and Keefer (1992)]. [b]Estimated using Eq. (5) of [Jibson and Keefer (1992)].

1811–12 events, several existing strong-motion records have shaking characteristics similar enough to the estimated shaking characteristics of the 1811–12 events to be useful. An extensive catalog of digitized strong-motion records was examined, primarily from California earthquakes, and two records for each of the three 1811–12 earthquakes were selected. Records were chosen to match, as closely as possible, the estimated range of Arias intensities and PGAs from the 1811–12 events so as to bracket the likely ranges of shaking conditions that actually occurred. None of the available strong-motion records have Arias intensities greater than 10 m/s; therefore, where estimated Arias intensities exceeded this level, the available record having the greatest Arias intensity was used. Table 3 shows the records selected and compares some of their characteristics with those estimated by Jibson and Keefer (1993) for the Stewart site from the 1811–12 earthquakes.

### 5.4.4. Calculation of the Newmark landslide displacement

Critical accelerations were calculated based on a thrust angle of 16° and on the factors of safety

(FS 1.62, 1.64) of the two circular slip surfaces in the perched and sloped ground-water conditions. These slip surfaces most closely coincide with the actual surface and have the lowest factors of safety. Eq. (1) yields critical accelerations of 0.17–0.18 $g$ for these input values. These critical accelerations are specified in the computer program that double integrates the strong-motion record to calculate the Newmark displacement.

The significance of the Newmark displacements must be judged in terms of the probable effect on the potential landslide mass. For example, Wieczorek et al. (1985) used 5 cm as the critical displacement leading to failure of landslides in San Mateo County, CA; Keefer and Wilson (1989) used 10 cm as the critical displacement for coherent slides in southern California. When displacements in this range occur, previously undisturbed soils can lose some of their strength and be in a residual-strength condition. Static factors of safety using residual shear strengths can then be calculated to determine the stability of the landslide after earthquake shaking (and consequent inertial landslide displacement) ceases.

Table 3 shows Newmark displacements calcu-

lated for the two critical accelerations using the six strong-motion records listed. Displacements are 6–55 cm and thus fall on both sides of the critical 5–10 cm range. Displacements generated by the model earthquakes of the 16 December 1811 event are 6–8 cm; in this range, the likelihood of catastrophic failure is uncertain. The soils sampled and tested at the Stewart site all showed significant strength reductions during strain in both drained and undrained conditions (Jibson, 1985); residual strength generally was reached after shear displacements of about 0.5 cm (for silts and sands) to 6 cm (for clayey silts). Therefore, even modest displacements would have at least partially reduced the soil shear strength and thus would have reduced the critical acceleration of the landslide in future earthquakes. The model earthquakes for the 23 January and 7 February 1812 events generated Newmark displacements of 23–55 cm, which undoubtedly would have reduced soil shear strengths to residual levels.

For all ground-water conditions, static factors of safety for the Stewart slide calculated using residual shear strengths in both drained and undrained conditions (Jibson, 1985) all were less than 0.8 and in most cases were less than 0.4. Therefore, if the bluff materials reach residual strength, catastrophic failure almost certainly will occur. Displacements of 20–50 cm thus would reduce the shear strength of the bluff materials to a residual-strength condition and probably would lead to catastrophic failure. The repeated shaking of the bluffs by three large earthquakes (and the far more numerous moderate earthquakes) and the reduction of the critical acceleration of the partially failed landslide mass leave little doubt that very large displacements of the Stewart slide would have occurred during the entire 1811–12 earthquake sequence.

### 5.4.5. Summary

In summary, static stability analyses of drained conditions indicate that failure of the Stewart landslide in aseismic conditions is highly unlikely. Dynamic analysis shows that shaking conditions similar to those in 1811–12 would have induced large displacements that probably would lead to catastrophic failure. Further analysis (Jibson and

Keefer, 1993) showed that no earthquakes since 1812 could have triggered the observed landslide movement. The results of these analyses are consistent with results from field and regional studies (Jibson and Keefer, 1988, 1989), which indicated that the ages and regional distribution of landslides similar to the Stewart slide are consistent with triggering in 1811–12. Datable material needed to determine a precise age of landsliding at the Stewart site could not be recovered, so the analytical approach outlined above was crucial in linking the landslide to the 1811–12 earthquakes. Considered together, these studies strongly support such a conclusion.

The reliability of results of analyses such as this obviously depends on the amount and quality of input data and the appropriateness and accuracy of the modeling approach used. As Clark and Cole (1992) pointed out, obtaining samples that accurately reflect the shear strength along a failure plane is very difficult, particularly in cases where reactivated landslides having well-formed basal shear surfaces are being analyzed. In such cases, using minimum shear-strength estimates is generally appropriate because the material along the pre-existing shear surface is probably at residual level (Clark and Cole, 1992).

### 5.5. Analysis of unknown seismic conditions

The procedure described above was used to test the hypothesis that an individual landslide was triggered by a historical earthquake whose magnitude and location have already been estimated. The goal of most paleoseismic investigations, by contrast, is to detect and characterize prehistoric or undocumented earthquakes whose effects are recorded in the geological record. Therefore, a more general procedure for paleoseismic landslide analysis is required.

If static stability analyses clearly indicate that failure in aseismic conditions is highly unlikely, then an earthquake origin can be hypothesized on that basis alone. A dynamic analysis can then be used to estimate the minimum shaking intensities necessary to have caused failure. Such an approach requires a general relationship between critical acceleration, shaking intensity, and Newmark dis-

placement; a relationship developed by Jibson and Keefer (1993) is reiterated here.

Jibson and Keefer (1993) selected 11 strong-motion records having Arias intensities between 0.2 and 10.0 m/s, which span the range between the smallest shaking intensities that might cause landslide movement and the largest shaking intensities ever recorded. For each strong-motion record, they calculated the Newmark displacement for several critical accelerations between 0.02 and 0.40 g, the range of practical interest for most earthquake-induced landslides. Analysis of the resulting data set indicated that a multivariate model of the following form would fit the data well:

$$\log D_N = A \log I_a + B a_c + C \pm \sigma, \tag{3}$$

where $D_N$ is Newmark displacement in centimeters; $I_a$ is Arias Intensity in meters per second; $a_c$

is critical acceleration in $g$; $\sigma$ is the estimated standard deviation of the model; and $A$, $B$, and $C$ are the regression coefficients. The resulting model has an $R^2$ of 0.87, and the coefficients all are significant above the 99.9% confidence level:

$$\log D_N = 1.460 \log I_a - 6.642 a_c + 1.546 \pm 0.409 \tag{4}$$

This model yields the mean value of Newmark displacement when $\sigma$ is ignored; the variation about this mean represented by $\sigma$ results from the stochastic nature of earthquake ground shaking. Thus, even two strong-motion records having identical Arias intensities can produce significantly different Newmark displacements for slopes having identical critical accelerations. Therefore, Eq. (4) yields a range of displacement values that must be interpreted with considerable judgment. Fig. 8
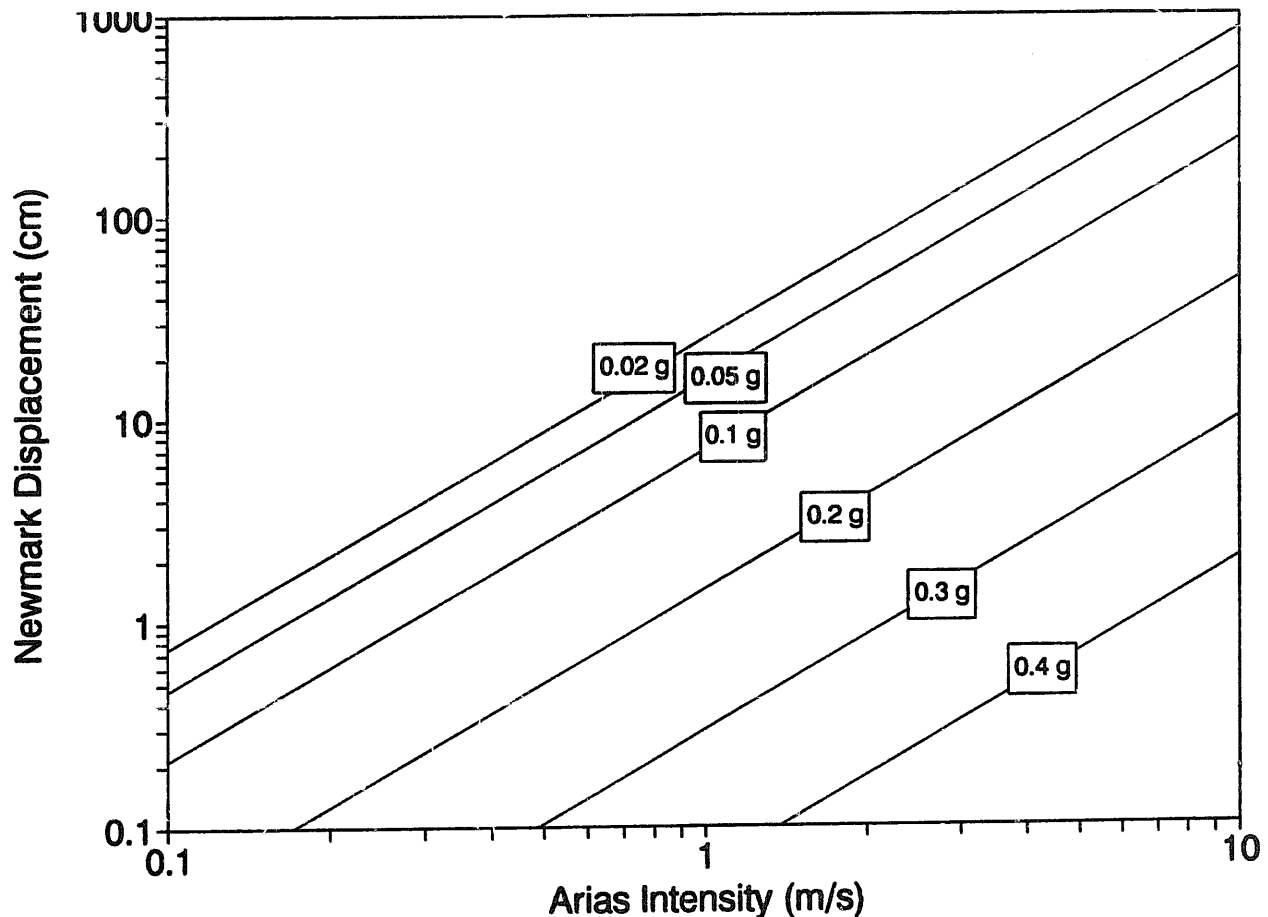


Fig. 8. Newmark displacement as a function of Arias intensity for several values of critical acceleration as modeled by Eq. (4).

shows the relation between Arias Intensity, critical acceleration, and Newmark displacement as defined by Eq. (4). The model underestimates Newmark displacement at low levels of Arias intensity (less than 0.5 m/s) for very small critical accelerations (0.02 $g$), but otherwise, the data are well fit by the model.

In the case of the Stewart landslide, if we knew nothing of the shaking history of the site, the minimum earthquake shaking intensity could be estimated using Eq. (4). This requires judging the amount of Newmark displacement (the critical displacement) that would reduce shear strength on the failure surface to residual levels and lead to catastrophic failure. As discussed previously, critical displacements of about 10 cm are probably realistic for this type of slide, based on previous studies (Wieczorek et al., 1985; Wilson and Keefer, 1985; Keefer and Wilson, 1989), laboratory shear-strength testing of soil samples from the site (Jibson, 1985), and field studies of landslides in the region (Jibson and Keefer, 1988). Inserting a Newmark displacement value of 10 cm and the range of critical accelerations of the Stewart landslide (0.17–0.18 $g$) into Eq. (4) yields a lower-bound Arias intensity of about 2.6 m/s to trigger failure and large continuing displacement of the Stewart slide.

Wilson and Keefer (1985) developed an empirical relationship between Arias intensity, earthquake magnitude, and source distance:

$$\log I_a = M - 2 \log R - 4.1, \tag{5}$$

where $I_a$ is Arias intensity in m/s, M is moment magnitude, and $R$ is earthquake source distance in km. For a minimum source distance of 5 km (focal depth at the epicenter), the Arias intensity of 2.6 m/s estimated above yields M = 5.9 as the minimum threshold earthquake magnitude required to have caused slope failure. Although this magnitude is considerably lower than those estimated to have been generated by the 1811–12 earthquakes, it provides a reasonable lower bound in the absence of any other information. If more than one landslide of identical age were similarly analyzed in an area, magnitude and location estimates could be optimized by using the larger

required source distances between two or more separate sites.

## 6. Interpreting results of paleoseismic landslide studies

Once a landslide or group of landslides has been identified, dated, and linked to earthquake shaking, what can we learn about the magnitude and location of the triggering earthquake? Several approaches to this last level of paleoseismic interpretation are possible, and, in most cases, multiple lines of evidence will be required to reasonably estimate magnitude and location. Perhaps the most important aspect of such interpretation is a thorough understanding of the characteristics of landslides triggered by recent, well-documented earthquakes.

### 6.1. Some characteristics of landslides triggered by earthquakes

Keefer (1984) conducted by far the most comprehensive study of landslides caused by historical earthquakes. He documented minimum earthquake magnitudes and intensities that have triggered landslides of various types, average and maximum areas affected by landslides as a function of magnitude, and maximum distances of landslides from earthquake sources as a function of magnitude. For these comparisons, he grouped different types of landslides into three categories: disrupted slides and falls (defined as falls, slides, and avalanches in rock and soil); coherent slides (defined as slumps and block slides in rock and soil and slow earth flows); and lateral spreads and flows (defined as lateral spreads and rapid flows in soil and subaqueous landslides).

### 6.1.1. Minimum earthquake magnitudes that trigger landslides

In a review of intensity reports from 300 earthquakes, Keefer (1984) found that the smallest earthquake reported to have caused landslides had a magnitude of 4.0. Landslides of various types have threshold magnitudes ranging from 4.0 to 6.5 (Table 4); disrupted landslides have lower thresh-

Table 4
Minimum earthquake magnitudes required to trigger landslides

| Earthquake magnitude | Type of landslide |
|---|---|
| 4.0 | Rock falls, rock slides, soil falls, disrupted soil slides |
| 4.5 | Soil slumps, soil block slides |
| 5.0 | Rock slumps, rock block slides, slow earth flows, soil lateral spreads, rapid soil flows, subaqueous landslides |
| 6.0 | Rock avalanches |
| 6.5 | Soil avalanches |

Data from [Keefer (1984)].

old magnitudes than coherent slides. Although smaller earthquakes could conceivably trigger landslides, such triggering by very weak shaking probably would occur on slopes where failure was imminent before the earthquake. And larger magnitudes are necessary to trigger numerous, widespread landslides.

### 6.1.2. Minimum shaking intensities that trigger landslides

Keefer (1984) also compared landslide initiation to Modified Mercalli Intensity (MMI). Table 5 shows the lowest MMI values and the predominant minimum MMI values reported where the three categories of landslides occurred. Keefer's (1984) data show that landslides of various types are triggered one to five levels lower than indicated in the current language of the MMI scale.

Nikonov (1988) and Solonenko (1977) correlated landslide initiation with threshold shaking levels using the Russian MSK intensity scale. Their

Table 5
Minimum modified Mercalli intensity required to trigger landslides

| Landslide type | Lowest modified Mercalli intensity | Predominant modified Mercalli intensity |
|---|---|---|
| Disrupted slides and falls | IV | VI |
| Coherent slides | V | VII |
| Lateral spreads and flows | V | VII |

Data from [Keefer (1984)].

observations indicated that small landslides are initiated at intensities IV–VII, large landslide at intensities VIII–IX, and "large landslides in basement rocks" at intensities of IX or greater.

### 6.1.3. Areas affected by earthquake-triggered landslides

For 30 historical earthquakes, Keefer (1984) drew boundaries around all reported landslide locations and calculated the areas enclosed. His plot of area versus earthquake magnitude (Fig. 9) shows a well-defined upper bound curve representing the maximum area that can be affected for a given magnitude. Also shown is a regression line showing average area, the equation of which is

$$\log A = M_S - 3.46, \tag{6}$$

where $A$ is area affected by landslides in km$^2$ and $M_S$ is earthquake surface-wave magnitude (Keefer and Wilson, 1989).

Keefer (1984) noted that the area affected by landslides will be influenced, in part, by the geological conditions that control the distribution of susceptible slopes. Also, he noted that earthquakes having focal depths greater than about 30 km plot on or near the upper bound (Fig. 9), which indicates that deeper earthquakes can trigger landslides over larger areas. Surprisingly, he found no differences in the areas affected by landsliding that could be attributed to regional differences in seismic attenuation.

### 6.1.4. Maximum distance of landslides from earthquake sources

For each of the three categories of landslides, Keefer (1984) related the triggering earthquake magnitude to the maximum distance from the earthquake epicenter and the closest point on the fault-rupture surface (Fig. 10). Again, upper bound curves are well defined and are constrained to pass through the minimum threshold magnitudes shown in Table 4 as distance approaches zero.

Fig. 10 indicates that disrupted slides and falls have the lowest shaking threshold and that lateral spreads and flows have the highest shaking threshold. As with area, earthquakes having focal depths greater than 30 km generally triggered landslides
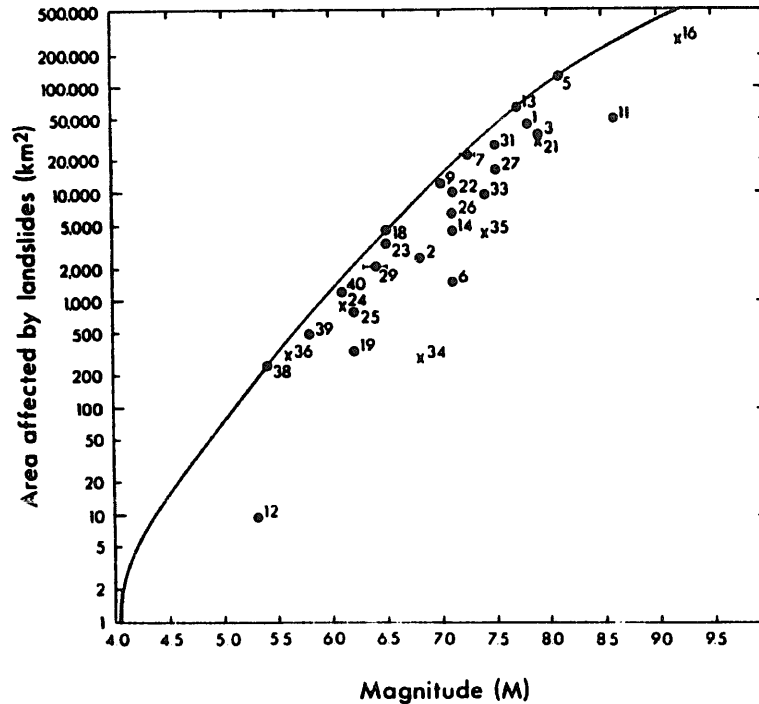
Fig. 9. Area affected by landslides in earthquakes having different (generally $M_s$) magnitudes (from Keefer, 1984). Solid line is upper bound; numbers beside data points refer to earthquakes analyzed by Keefer (1984); dots denote onshore earthquakes; x, offshore earthquakes.

at greater distances than shallower earthquakes of similar magnitude.

### 6.2. Interpreting earthquake magnitude, location, and shaking intensity

Keefer's results (Keefer, 1984) allow interpretation of earthquake magnitude and location in a variety of ways. If a single landslide is identified as being seismically triggered, then a minimum magnitude and MMI can be estimated based on the landslide type. For example, Schuster et al. (1992) used Keefer's magnitude (Keefer, 1984) of 6.5 as a lower bound estimate for triggering of rock avalanches that formed dams. If several landslides in an area are identified as being seismically induced, then application of Keefer's magnitude-area and magnitude-distance relationships (Keefer, 1984) can yield minimum magnitude estimates. As the area in which landslides documented to have been triggered by the same earthquake increases, the estimated magnitude will increase toward the actual magnitude of the triggering

earthquake. Therefore, documentation and analysis of landslides over a large area will produce more accurate magnitude estimates. If seismic source zones are well documented, then the distance from the closest source zone to the farthest landslide will yield a reasonable minimum magnitude estimate. The observation that greater source depth relates to greater areas affected and source distances for landslides of all types (Keefer, 1984) further complicates estimation of earthquake magnitude.

For a specific region, earthquake magnitude can be estimated based on comparison of paleoseismic landslide distribution with landslide distributions from recent, well-documented earthquakes in the region. This approach has been applied to landslide dams in New Zealand (Adams, 1981a) and to landslides in central Asia (Nikonov, 1988).

Several types of interpretations from seismically triggered turbidites are possible. The linear extent of synchronous turbidites triggered from the edges of continental shelves can be used to estimate fault rupture length and, hence, earthquake magnitude
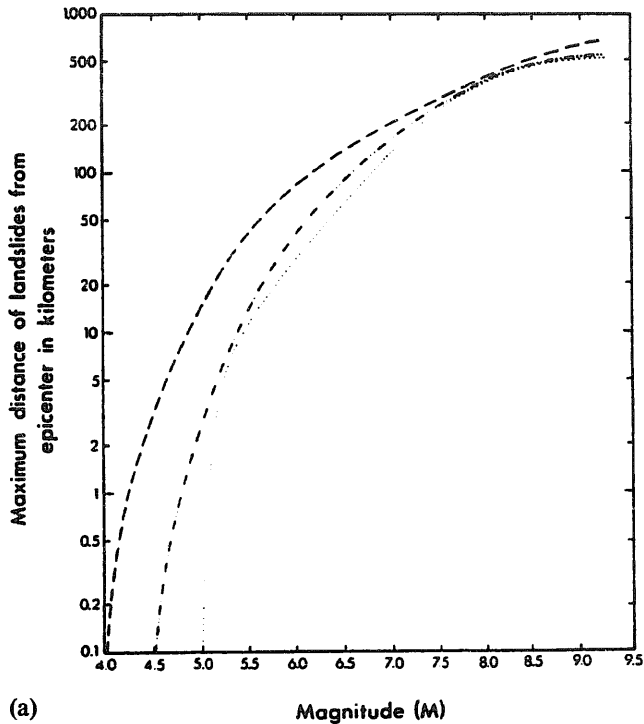
(a)
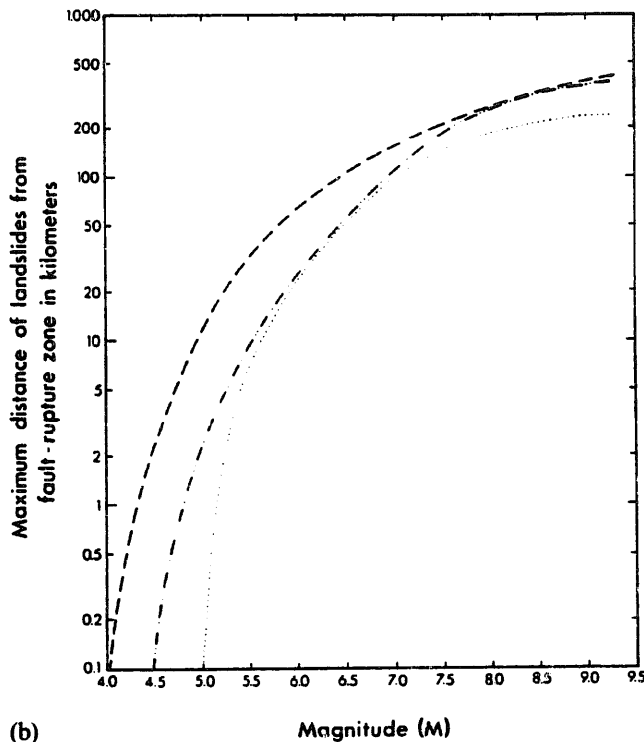


(b)

Fig. 10. Maximum distance to landslides from (A) epicenter and (B) fault-rupture zone for earthquakes of different magnitudes (from Keefer, 1984). Dashed line is upper bound for disrupted slides and falls; dash-double-dot line is upper bound for coherent slides; and dotted line is upper bound for lateral spreads and flows.

(Adams, 1990). The extreme size and very long recurrence intervals ($10^4$–$10^6$ years) for lithified turbidites preserved in the older geological record argue that they formed in very rare, large-magnitude earthquakes (Mutti et al., 1984; Spalletta and Vai, 1984). The paucity of seismically induced sedimentary structures in some older, lithified deposits likewise suggests long recurrence intervals and consequent large earthquake magnitudes (Seilacher, 1969).

Harp and Wilson (1989, 1995) developed seismic shaking-intensity thresholds for disrupted landslides by mapping the geographic limits of rock falls and rock slides triggered by two California earthquakes and comparing these limits with contours of instrumentally recorded shaking intensity. They found that Arias-intensity shaking thresholds for landslides in the Cenozoic rocks in the region were 0.08–0.60 m/s, and thresholds for landslides in pre-Cenozoic rocks were 0.01–0.07 m/s. Such thresholds allow estimation of minimum shaking intensities in areas where earthquakes have triggered landslides.

Static and dynamic slope-stability analyses facilitate direct estimation of the minimum ground shaking, and hence magnitude, required to have caused failure of individual landslides (Jibson and Keefer, 1992, 1993), as described in detail previously. If the critical acceleration of a landslide can be determined by stability analysis, and if a reasonable amount of displacement (such as 10 cm) leading to catastrophic failure can be estimated, then Eq. (4) can be used to estimate the threshold Arias intensity required to initiate failure. Eq. (5) (from Wilson and Keefer, 1985) can then be used to estimate the minimum magnitude of the triggering earthquake.

A similar approach for estimating earthquake magnitude from the results of slope-stability analyses was outlined by Crozier (1992) and is based on the work of Wilson and Keefer (1985). They defined a quantity referred to as $(A_c)_{10}$, which is the critical acceleration of a landslide that will yield 10 cm of displacement (the estimated critical displacement leading to catastrophic failure) in a given level of earthquake shaking. They selected 10 strong motion records that spanned a range of Arias intensities and iteratively determined $(A_c)_{10}$

for each record. From these values, they developed a regression model relating Arias intensity to $(A_c)_{10}$:

$$\log (A_c)_{10} = 0.79 \log I_a - 1.095, \qquad (7)$$

where $(A_c)_{10}$ is in $g$ and $I_a$ is in m/s. If the critical acceleration of a landslide can be determined, then this value can be used as the threshold value of $(A_c)_{10}$ in Eq. (7), and the Arias intensity that would trigger the critical displacement of 10 cm can be calculated. Magnitude can then be estimated from Eq. (5).

Stability analysis also could possibly be applied to speleothems, whose dynamic stability can easily be modeled, to estimate the ground shaking required to cause failure.

Earthquake locations generally are estimated based on the distribution of synchronous landslides attributed to a single seismic event. In a broad area of roughly similar susceptibility to landsliding, the earthquake epicenter probably will coincide fairly closely with the centroid of the landslide distribution. In areas of highly variable or asymmetrical landslide susceptibility, epicenter estimation is much more difficult and subject to error. In areas where seismic source zones are well defined, the epicentral location is best defined as the point in a known seismic source zone (or along a known seismogenic fault) closest to the centroid of the landslide distribution.

## 7. Some final comments

The use of landslides as paleoseismic indicators is a fairly recent development that is beginning to expand in scope and complexity. A few final comments on the advantages and limitations of paleoseismic landslide analysis are in order.

The primary limitation of paleoseismic analysis of landslides is the inherent uncertainty in interpreting a seismic origin. Unlike liquefaction, which can occur aseismically only in relatively rare conditions, landslides of all types form readily in the absence of earthquake shaking as a result of many different triggering mechanisms. In many cases, ruling out aseismic triggering will be impossible, and the level of confidence in any resulting paleo-

seismic interpretation will be limited. For this reason, paleoseismic landslide analysis should include, so far as possible, multiple lines of evidence to constrain a seismic origin. In this way, a strong case can be built for seismic triggering of one or more landslides, even if no single line of evidence is unequivocal. Where independent paleoseismic evidence from fault or liquefaction studies is available, paleoseismic landslide evidence can provide useful corroboration.

Detailed slope-stability analysis generally can be performed only on certain types of landslides. Failure conditions of falls, avalanches, and disrupted slides cannot easily be modeled using Newmark's method (Newmark, 1965), and even static stability analyses of these types of slides can be very problematic. Also, the pre-landslide geometry of slides in very steep terrain can be difficult or impossible to reconstruct. Thus, the analytical method described herein generally can be applied only to fairly coherent landslides where pre-landslide geometry can be reconstructed with confidence, where ground-water conditions can be modeled reasonably, and where the geotechnical properties of the materials can be accurately measured.

Even allowing for these limitations, paleoseismic landslide studies have been extremely useful where applied successfully, and they hold great potential in the field of paleoseismology. Dating landslide deposits is, in many cases, easier than dating movement along faults because many different dating methods can be used on the same slide to produce redundant results. In addition, landslides have the potential for preserving large amounts of datable material in the various parts of the slide (scarp, body, toe, etc.). In areas containing multiple or poorly defined seismic sources, paleoseismic ground-failure analysis may be preferable to fault studies because landslides preserve a record of the shaking history of a site or region from all seismic sources. Knowing the frequency of strong shaking events may, in many cases, be more critical than knowing the behavior of any individual fault.

Paleoseismic landslide analysis may have greatest utility in assessing earthquake hazards in stable continental interiors, such as the eastern and central United States, where fault exposures are

rare or absent but where earthquakes are known to have occurred. In such areas, analysis of earthquake-triggered ground failure, both landslides and liquefaction, may be one of the few paleoseismic tools available.

Another advantage of paleoseismic landslide analysis is that it gets directly at the effects of the earthquakes being studied. Ultimately, most paleoseismic studies are aimed at assessing earthquake hazards. Fault studies can be used to estimate slip rates, recurrence intervals, and, indirectly, magnitudes. From these findings, we extrapolate the effects of a possible earthquake on such a fault. In paleoseismic landslide studies, we observe the effects directly. Thus, if a seismic origin can be established, a landslide shows directly what the effects of some previous earthquake were. Even if magnitude and location are poorly constrained, at least we have a partial picture of the actual effects of seismic shaking in a locale or region. Thus, for example, a map of the distribution of landslides triggered by the 1811–12 earthquakes in the New Madrid seismic zone (Jibson and Keefer, 1988) yields a very useful picture of the likely distribution of landslides in future earthquakes there.

In conclusion, paleoseismic landslide analysis can be applied in a variety of ways and can yield many different types of results. Although interpretations are limited by the certainty with which a seismic origin can be established, paleoseismic landslide studies can play a vital role in the paleoseismic interpretation of many areas, particularly those lacking fault exposures.

## Acknowledgment

## References

Adam, D.P., 1975. A late Holocene pollen record from Pearson's Pond, Weeks Creek landslides, San Francisco Peninsula, California. US Geol. Surv. J. Res., 3: 721–731.

Adams, J., 1980. Contemporary uplift and erosion of the Southern Alps, New Zealand: Summary. Geol. Soc. Am. Bull., Part I, 91: 2–4.

Adams, J., 1981a. Earthquake-dammed lakes in New Zealand. Geology, 9: 215–219.

Adams, J., 1981b. Earthquakes, landslides, and large dams in New Zealand. Bull. NZ Natl. Soc. Earthquake Eng., 14(2): 93–95.

Adams, J., 1990. Paleoseismicity of the Cascadia subduction zone: Evidence from turbidites off the Oregon-Washington margin. Tectonics, 9: 569–583.

Allen, J.R.L., 1986. Earthquake magnitude-frequency, epicentral distance, and soft-sediment deformation in sedimentary basins. Sedimentary Geol., 46: 67–75.

Andrews, D.J. and Bucknam, R.C., 1987. Fitting degradation of shoreline scarps by a model with nonlinear diffusion. J. Geophys. Res., 92: 12857–12867.

Andrews, D.J. and Hanks, T.C., 1985. Scarps degraded by linear diffusion: inverse solution for age. J. Geophys. Res., 90, 10193–10208.

Arias, A., 1970. A measure of earthquake intensity. In Hansen, R.J., ed., Seismic design for nuclear power plants. Cambridge, Massachusetts Institute of Technology Press, pp. 438–483.

Atwater, B.F., 1987. Evidence of great Holocene earthquakes along the outer coast of Washington State. Science, 236, 942–944.

Beck, A.C., 1968. Gravity faulting as a mechanism of topographic adjustment. NZ J. Geol. Geophys., 11, 191–199.

Bégin, C. and Filion, L., 1985. Analyse dendrochronologique d'un glissement de terrain de la région du Lac à l'Eau Claire (Québec nordique). Can J. Earth Sci., 22, 175–182 (in French).

Birkeland, P.W., 1984. Soils and geomorphology. New York, Oxford University Press, 372 pp.

Birkeland, P.W., Machette, M.N. and Haller, K.M., 1991. Soils as a tool for applied Quaternary geology. Utah Geological and Mineral Survey Miscellaneous Publication 91-3, 63 pp.

Bovis, M.J., 1982. Uphill-facing (antislope) scarps in the Coast Mountains, southwest British Columbia. Geol. Soc. Am. Bull., 93: 804–812.

Brune, J.N., 1996. Precariously balanced rocks and ground-motion maps for southern California. Bull. Seismol. Soc. Am., 86(1A): 43–54.

Brunsden, D. and Prior, D.B., 1984. Slope instability. New York, John Wiley and Sons, 620 pp.

Bucknam, R.C. and Anderson, R.E., 1979. Estimation of fault-scarp ages from a scarp-height–slope-angle relationship. Geology, 7: 11–14.

Bull, W.B., 1996. Prehistorical earthquakes on the Alpine fault, New Zealand. J. Geophys. Res., 101(B3): 6037–6050.

Bull, W.B., Cowan, H.A. and Pettinga, J.R., 1991. New ways of dating earthquakes on two segments of the oblique-slip Hope fault, New Zealand. Geol. Soc. Am., Abstracts with Programs, 23(5): A431.

Burrows, C.J., 1975. A 500-year-old landslide in the Acheron River valley, Canterbury (Note). NZ J. Geol. Geophys., 18: 357–360.

Chinn, T.J.H., 1981. Use of rock weathering-rind thickness for Holocene absolute age-dating in New Zealand. Arctic Alpine Res., 13: 33–45.

Christiansen, E.A., 1983. The Denholm landslide, Saskatchewan. Part I: Geology. Can. Geotech. J., 20: 197–207.

Clark, B.R. and Cole, W.F., 1992. Importance of accurate geological characterization in the analysis of seismically triggered landslides. In: M.L. Stout (Editor), Proceedings of the 35th Annual Meeting of the Association of Engineering Geologists, Long Beach, CA, pp. 469–472.

Colman, S.M. and Watson, K., 1983. Ages estimated from a diffusion equation model for scarp degradation. Science, 221, 263–265.

Conrad, T.A., 1856. Observations of the Eocene deposit of Jackson, Miss., with descriptions of 34 new species of shells and corals. Philadelphia Academy of Natural Sciences, Proceedings, 1855, 1st ser., 7: 257–258.

Costa, J.E. and Schuster, R.L., 1991. Documented historical landslide dams from around the world. US Geological Survey Open-File Report 91-239, 486 pp.

Crozier, M.J., 1992. Determination of paleoseismicity from landslides. In: D.H. Bell (Editor), Landslides (Glissements de terrain), International Symposium, 6th, Christchurch, New Zealand, 1992, Proceedings: Rotterdam, A.A. Balkema, 2: 1173–1180.

Dietrich, W.E. and Dorn, R., 1984. Significance of thick deposits of colluvium on hillslopes: A case study involving the use of pollen analysis in the coastal mountains of northern California. J. Geol., 92: 147–158.

Dobry, R., Idriss, I.M. and Ng, E., 1978. Duration characteristics of horizontal components of strong-motion earthquake records. Bull. Seismol. Soc. Am., 68: 1487–1520.

Doig, R., 1986. A method for determining the frequency of large-magnitude earthquakes using lake sediments. Can. J. Earth Sci., 23: 930–937.

El-Isa, Z.H. and Mustafa, H., 1986. Earthquake deformations in the Lisan deposits and seismotectonic implications. Royal Astronom. Soc. Geophys. J., 86: 413–424.

Field, M.E., Gardner, J.V., Jennings, A.E. and Edwards, B.D., 1982. Earthquake-induced sediment failures on a 0.25° slope, Klamath River delta, California. Geology, 10: 542–546.

Forti, P. and Postpischl, D., 1984. Seismotectonic and paleoseismic analyses using karst sediments. Mar. Geol., 55: 145–161.

Franks, J.W. and Johnson, R.H., 1964. Pollen analytical dating of a Derbyshire landslide. New Phytol., 63: 209–216.

Fuller, M.L., 1912. The New Madrid earthquake. US Geol. Surv. Bull. 494, 120 pp.

Gedney, D.S. and Weber, W.G., Jr., 1978. Design and construction of soil slopes. In: R.L. Schuster and R.J. Krizek (Editors), Landslides – Analysis and Control: Transportation Research Board, National Academy of Sciences, Washington, DC, Special Report 176, pp. 172–191.

Goodman, R.E. and Seed, H.B., 1966. Earthquake-induced dis-

placements in sand embankments. American Society of Civil Engineers. J. Soil Mech. Found. Div., 92(SM2): 125–146.

Hadley, D.M., Hawkins, H.G. and Benuska, K.L., 1983. Strong ground motion record of the 16 September 1978 Tabas, Iran, earthquake. Bull. Seismol. Soc. Am., 73(1): 315–320.

Hamilton, R.M. and Johnston, A.C., 1990. Tecumseh's prophecy – Preparing for the next New Madrid earthquake. US Geol. Surv. Circ. 1066, 30 pp.

Hansen, W.R., 1965. Effects of the earthquake of March 27, 1964, at Anchorage, Alaska. US Geol. Surv. Professional Paper 542-A, 68 pp.

Hanks, T.C. and Johnston, A.C., 1992. Common features of the excitation and propagation of strong ground motion for North American earthquakes. Bull. Seismol. Soc. Am., 82: 1–23.

Harp, E.L. and Wilson, R.C., 1989. Shaking intensity thresholds for seismically induced landslides. Geol. Soc. Am. Abstracts with Programs, 21(5): 90.

Harp, E.L. and Wilson, R.C., 1995. Shaking intensity thresholds for rock falls and slides: evidence from 1987 Whittier Narrows and Superstition Hills earthquake strong-motion records. Bull. Seismol. Soc. Am., 85: 1739–1757.

Heezen, B.C. and Ewing, M., 1952. Turbidity currents and submarine slumps, and the 1929 Grand Banks earthquake. Am. J. Sci., 250: 849–873.

Hempton, M.R. and Dewey, J.F., 1983. Earthquake-induced deformational structures in young lacustrine sediments, East Anatolian Fault, southeast Turkey. Tectonophysics, 98: T7–T14.

Hunt, C.B., 1975. Death Valley: Geology, Ecology, and Archeology. Berkeley, University of California Press, 234 pp.

Hupp, C.R., Osterkamp, W.R. and Thornton, J.L., 1987. Dendrogeomorphic evidence and dating of recent debris flows on Mount Shasta, northern California. US Geol. Surv. Professional Paper 1396-B, 39 pp.

Jacoby, G.C., Williams, P.L. and Buckley, B.M., 1992. Tree ring correlation between prehistoric landslides and abrupt tectonic events in Seattle, Washington. Science, 258: 1621–1623.

Jahn, A., 1964. Slopes morphological features resulting from gravitation. Zschr. Geomorphol, Suppl., 5: 59–72.

Jensen, J.M., 1983. The Upper Gros Ventre landslide of Wyoming: A dendrochronology of landslide events and the possible mechanics of failure. Geol. Soc. Am., Abstracts with Programs, 15(5): 387.

Jibson, R.W., 1985. Landslides caused by the 1811–12 New Madrid earthquakes. Stanford, CA, Stanford University, Ph.D. dissertation, 232 pp.

Jibson, R.W., 1993. Predicting earthquake-induced landslide displacements using Newmark's sliding block analysis. Transportation Res. Record no. 1411: 9–17.

Jibson, R.W. and Keefer, D.K., 1988. Landslides triggered by earthquakes in the central Mississippi Valley, Tennessee and Kentucky. US Geol. Surv. Professional Paper 1336-C, 24 pp.

Jibson, R.W. and Keefer, D.K., 1989. Statistical analysis of factors affecting landslide distribution in the New Madrid

seismic zone, Tennessee and Kentucky. Eng. Geol., 27: 509–542.

Jibson, R.W. and Keefer, D.K., 1992. Analysis of the seismic origin of a landslide in the New Madrid seismic zone. Seismol. Res. Lett., 63: 427–437.

Jibson, R.W. and Keefer, D.K., 1993. Analysis of the seismic origin of landslides – Examples from the New Madrid seismic zone. Geol. Soc. Am. Bull., 105: 421–436.

Jibson, R.W., Prentice, C.S., Borissoff, B.A., Rogozhin, E.A. and Langer, C.J., 1994. Some observations of landslides triggered by the 29 April 1991 Racha earthquake, Republic of Georgia. Bull. Seismol. Soc. Am., 84: 963–973.

Johnson, R.H., 1987. Dating of ancient, deep-seated landslides in temperate regions. In: M.G. Anderson and K.S. Richards (Editors), Slope Stability: New York, John Wiley and Sons, pp. 561–600.

Jones, G.D.B. and Thompson, F.H., 1965. Excavations at Mam Tor and Brough-en-Noe. Derbyshire Archeol. J., 85: 89–93.

Kastens, K.A., 1984. Earthquakes as a triggering mechanism for debris flows and turbidites on the Calabrian ridge. Mar. Geol., 55: 13–33.

Keefer, D.K., 1984. Landslides caused by earthquakes. Geol. Soc. Am. Bull., 95: 406–421.

Keefer, D.K. and Wilson, R.C., 1989. Predicting earthquake-induced landslides, with emphasis on arid and semi-arid environments In: P.M. Sadler and D.M. Morton (Editors), Landslides in a Semi-Arid Environment: Riverside, CA, Inland Geological Society, 2: 118–149.

Keefer, D.K., Wilson, R.C., Harp, E.L. and Lips, E.W., 1985. The Borah Peak, Idaho earthquake of October 28, 1983 – landslides. Earthquake Spectra, 2: 91–125.

Knuepfer, P.L.K., 1988. Estimating ages of late Quaternary stream terraces from analysis of weathering rinds and soils. Geol. Soc. Am. Bull., 100: 1224–1236.

Lambe, T.W. and Whitman, R.V., 1969. Soil Mechanics. New York, John Wiley and Sons, 553 pp.

Lee, H.J. and Edwards, B.D., 1986. Regional method to assess offshore slope stability. J. Geotech. Eng., 112: 489–509.

Logan, R.L. and Schuster, R.L., 1991. Lakes divided: The origin of Lake Crescent and Lake Sutherland, Clallam County, Washington. Washington Division of Geology and Earth Resources, Washington Geology, 19(1): 38–42.

Mayer, L., 1984. Dating Quaternary fault scarps in alluvium using morphological parameters. Quaternary Res., 22: 300–313.

McCalpin, J.P., 1984. Preliminary age classification of landslides for inventory mapping. Engineering Geology and Soils Engineering Symposium, 21st, University of Idaho, Moscow, Idaho, 1984, Proceedings, pp. 99–120.

McCalpin, J.P., 1986. Relative dating and age classification of landslides. Association of Engineering Geologists, Abstracts and Program, 29th Annual Meeting, San Francisco, pp. 56.

McCalpin, J.P., 1989. Prehistoric earthquake-induced landslides along the Awatere fault, South Island, New Zealand. Association of Engineering Geologists, Abstract and Program, 32nd Annual Meeting, Vail, Colorado, pp. 94.

McCalpin, J.P., 1992. Glacial and postglacial geology near Lake

Tennyson, Clarence River, New Zealand. NZ J. Geol. Geophys., 35: 201–210.

McCalpin, J.P. and Rice, J.B., Jr., 1987. Spatial and temporal analysis of 1200 landslides in a 900 km$^2$ area, middle Rocky Mountains. In: International Conference and Field Workshop on Landslides, 5th, Christchurch, New Zealand, 1987, Proceedings, pp. 137–146.

McGee, W.J., 1891. The Lafayette Formation. US Geological Survey 12th Annual Report, pt. 1, pp. 387–521.

Morton, D.M. and Sadler, P.M., 1989. Landslides flanking the northeastern Peninsular Ranges and in the San Gorgonio Pass area of southern California. In: P.M. Sadler and D.M. Morton (Editors), Landslides in a Semi-arid Environment. Riverside, CA, Inland Geological Society, 2: 338–355.

Mutti, E., Lucchi, F.R., Seguret, M. and Zanzucchi, G., 1984. Seismoturbidites: A new group of resedimented deposits. Mar. Geol., 55: 103–116.

Nash, D.B., 1980. Morphological dating of degraded normal fault scarps. J. Geol., 88: 353–360.

Naumann, C.M. and Savigny, K.W., 1992. Large rock avalanches and seismicity in southwestern British Columbia, Canada. In: D.H. Bell (Editor), Landslides (Glissements de terrain), International Symposium, 6th, Christchurch, New Zealand, 1992, Proceedings: Rotterdam, A.A. Balkema, 2: 1187–1192.

Newmark, N.M., 1965. Effects of earthquakes on dams and embankments. Geotechnique, 15(2): 139–160.

Nikonov, A.A., 1988. Reconstruction of the main parameters of old large earthquakes in Soviet Central Asia using the paleoseismogeological method. Tectonophysics, 147: 297–312.

Nikonov, A.A. and Shebalina, T.Y., 1979. Lichenometry and earthquake age determination in central Asia. Nature, 280: 675–677.

Nuttli, O.W., 1973. The Mississippi Valley earthquakes of 1811 and 1812: Intensities, ground motion, and magnitudes. Seismol. Soc. Am. Bull., 63: 227–248.

Nuttli, O.W., 1983. Average seismic source-parameter relations for mid-plate earthquakes. Bull. Seismol. Soc. Am., 73(2): 519–535.

Oelfke, J.G. and Butler, D.R., 1985. Lichenometric dating of calcareous landslide deposits, Glacier National Park, Montana. Northwest Geol., 17: 7–10.

Osterkamp, W.R. and Hupp, C.R., 1987. Dating and interpretation of debris flows by geologic and botanical methods at Whitney Creek Gorge, Mount Shasta, California. In: J.E. Costa and G.F. Wieczorek (Editors), Debris flows/avalanches: Process, recognition, and mitigation: Geological Society of America. Rev. Eng. Geol., 7: 157–164.

Perissoratis, C., Mitropoulos, D. and Angelopoulos, I., 1984. The role of earthquakes in inducing sediment mass movements in the eastern Korinthiakos Gulf. An example from the February 24–March 4, 1981 activity. Mar. Geol., 55: 35–45.

Perrin, N.D. and Hancox, G.T., 1992. Landslide-dammed lakes in New Zealand – Preliminary studies on their distribution, causes and effects. In: D.H. Bell (Editor), Landslides (Glisse-

ments de terrain), International Symposium, 6th, Christchurch, New Zealand, 1992, Proceedings: Rotterdam, A.A. Balkema, 2: 1457–1466.

Plaziat, J.C., Purser, B.H. and Philobbos, E., 1990. Seismic deformation structures (seismites) in the syn-rift sediments of the NW Red Sea (Egypt). Bull. Soc. Géol. France, ser. 8, 6: 419–434.

Potter, P.E., 1955. The petrology and origin of the Lafayette Gravel, part II, geomorphic history. J. Geol., 63(2): 115–132.

Pratt, B.R., 1992. Shrinkage features ("molar tooth" structure) in Proterozoic limestones-New model for their origin through synsedimentary earthquake-induced dewatering (abstract). Geol. Soc. Am., Abstracts with Programs, 24(7): 53.

Pratt, B.R., 1994. Seismites in the Mesoproterozoic Altyn Formation (Belt Supergroup), Montana: A test for tectonic control of peritidal carbonate cyclicity. Geology, 22: 1091–1094.

Reeder, J.W., 1979. The dating of landslides in Anchorage, Alaska – A case for earthquake-triggered movements. Geol. Soc. Am., Abstracts with Programs, 11(7): 501.

Rojstaczer, S. and Wolf, S., 1992. Permeability changes associated with large earthquakes: an example from Loma Prieta, California. Geology, 20: 211–214.

Schroder, J.F., Jr., 1970. Landslide landforms and the concept of geomorphic age applied to landslides. International Geographic Congress, Commun. no. 21, Selected Papers, vol. 1, Physical Geography, pp. 124–126.

Schuster, R.L. and Krizek, R.J. (Editors), 1978. Landslides – Analysis and control: Transportation Research Board, National Academy of Sciences, Washington, DC, Special Report 176, 234 pp.

Schuster, R.L., Logan, R.L. and Pringle, P.T., 1992. Prehistoric rock avalanches in the Olympic Mountains, Washington. Science, 258: 1620–1621.

Seed, H.B., 1968. Landslides during earthquakes due to soil liquefaction. American Society of Civil Engineers. J. Soil Mech. Found. Div., 94: 1055–1122.

Seed, H.B., 1979. Considerations in the earthquake-resistant design of earth and rockfill dams. Geotechnique, 29(3): 215–263.

Seguret, M., Labaume, P. and Madariaga, R., 1984. Eocene seismicity in the Pyrenees from megaturbidites on the South Pyrenean Basin, Spain. Mar. Geol., 55: 117–131.

Seilacher, A., 1969. Fault-graded beds interpreted as seismites. Sedimentology, 13: 155–159.

Seilacher, A., 1984. Sedimentary structures tentatively attributed to seismic events. Mar. Geol., 55: 1–12.

Siegel, R.A., 1978. STABL user manual. West Lafayette, Indiana, Purdue University, 104 pp.

Sims, J.D., 1973. Earthquake-induced structures in sediments of Van Norman Lake, San Fernando, California. Science, 182: 161–163.

Sims, J.D., 1975. Determining earthquake recurrence intervals from deformational structures in young lacustrine sediments. Tectonophysics, 29: 141–152.

Small, R.J. and Clark, M.J., 1982. Slopes and weathering. Cambridge, Great Britain, Cambridge University Press, 112 pp.

Smirnova, T.Y. and Nikonov, A.A., 1990. A revised lichenometric method and its application dating great past earthquakes. Arctic Alpine Res., 22: 375–388.

Solonenko, V.P., 1977. Landslides and collapses in seismic zones and their prediction. Bull. Int. Assoc. Eng. Geol., no. 15: 4–8.

Spalletta, C. and Vai, G.B., 1984. Upper Devonian intraclast parabreccias interpreted as seismites. Mar. Geol., 55: 133–144.

Stout, M.L., 1969. Radiocarbon dating of landslides in southern California and engineering geology implications. In: S.A. Schumm and W.C. Bradley (Editors), United States contributions to Quaternary research: Geological Society of America Special Paper 123: 167–179.

Stout, M.L., 1977. Radiocarbon dating of landslides in southern California. California Division of Mines and Geology, California Geology, May 1977, pp. 99–105.

Tabor, R.W., 1971. Origin of ridge-top depressions by large-scale creep in the Olympic Mountains, Washington. Geol. Soc. Am. Bull., 82: 1811–1822.

Tallis, J.H. and Johnson, R.H., 1980. The dating of landslides in Longdendale, north Derbyshire, using pollen-analytical techniques. In: R.A. Cullingford, D.A. Davidson and J. Lewin (Editors), Timescales in Geomorphology. New York, John Wiley and Sons, pp. 189–205.

Terasmae, J., 1975. Dating of landslides in the Ottawa River valley by dendrochronology – A brief comment. In: E. Yatsu, A.J. Ward and F. Adams (Editors), Mass Wasting: Proceedings of the 4th Guelph Symposium on Geomorphology. Norwich, England, GeoAbstracts, pp. 153–158.

Tibaldi, A., Ferrari, L. and Pasquarè, G., 1995. Landslides triggered by earthquakes and their relations with faults and mountain slope geometry: an example from Ecuador. Geomorphology, 11: 215–226.

Varnes, D.J., 1978. Slope movement types and processes. In: R.L. Schuster and R.J. Krizek (Editors), Landslides – Analysis and control. Transportation Research Board, National Academy of Sciences, Washington, DC, Special Report 176, pp. 11–33.

Varnes, D.J., Radbruch-Hall, D.H. and Savage, W.Z., 1989. Topographic and structural conditions in areas of gravitational spreading of ridges in the western United States. US Geol. Surv. Professional Paper 1496, 28 pp.

Whitehouse, I.E. and Griffiths, G.A., 1983. Frequency and hazard of large rock avalanches in the central Southern Alps, New Zealand. Geology, 11: 331–334.

Wieczorek, G.F., 1984. Preparing a detailed landslide-inventory map for hazard evaluation and reduction. Bull. Assoc. Eng. Geol., 21: 337–342.

Wieczorek, G.F., Wilson, R.C. and Harp, E.L., 1985. Map showing slope stability during earthquakes of San Mateo County, California. US Geological Survey Miscellaneous Geologic Investigations Map I-1257E, scale 1:62,500.

Williams, P.L., Jacoby, G.C. and Buckley, B., 1992. Coincident

ages of large landslides in Seattle's Lake Washington. Geol. Soc. Am., Abstracts with Programs, 24(5): 90.

Wilson, R.C. and Keefer, D.K., 1983. Dynamic analysis of a slope failure from the 6 August 1979 Coyote Lake, California, earthquake. Seismol. Soc. Am. Bull., 73(3): 863–877.

Wilson, R.C. and Keefer, D.K., 1985. Predicting areal limits of earthquake-induced landsliding. In: J.I. Ziony (Editor), Evaluating Earthquake Hazards in the Los Angeles Region – An Earth-science Perspective. US Geol. Surv. Professional Paper 1360, pp. 316–345.

Wood, S.H., 1985. Regional increase in groundwater discharge after the 1983 Idaho earthquake: coseismic strain release,

tectonic and natural hydraulic fracturing. In: R.S. Stein and R.C. Bucknam (Editors), Proceedings of Workshop XXVIII on the Borah Peak, Idaho, earthquake, Volume A. US Geological Survey Open-File Report 85-290, pp. 573–592.

Yarnold, J.C. and Lombard, J.P., 1989. A facies model for large rock-avalanche deposits formed in dry climates. In: I.P. Colburn, P.L. Abbott and J. Minch (Editors), Conglomerates in Basin Analysis: A Symposium Dedicated to A.O. Woodford. Pacific Section, Society of Economic Paleontologists and Mineralogists, 62: 9–31.

Záruba, Q. and Mencl, V., 1982. Landslides and their control (2d edn.). Amsterdam, Elsevier, 324 pp.